Partial photodisintegration cross sections of *sd*-shell nuclei extracted from proton and deexcitation gamma-ray spectrometry

B. S. Ishkhanov and I. M. Kapitonov
Institute of Nuclear Physics, Moscow State University

R. A. Éramzhyan
Institute of Nuclear Research, Russian Academy of Sciences, Moscow

Fiz. Élem. Chastits At. Yadra **26**, 873–931 (July–August 1995)

A systematization of the partial transitions from the nucleon decay of the giant photonuclear resonance is presented. Data from experiments on both particle spectrometry and spectroscopy of secondary photons from the $(\gamma,x\gamma')$ reaction are used. More than 300 transitions in 15 nuclei of the *sd* shell ($8\leqslant Z\leqslant 20$) are analyzed. The semidirect part of the reaction is estimated. The role of nucleons that occupy different shells of the target nucleus is discussed. © *1995 American Institute of Physics.*

1. INTRODUCTION

In a previous review,[1] for three particular nuclei, we demonstrated the great effectiveness of the method of studying photodisintegration of nuclei that is based on measurement of the spectrum of γ rays from deexcitation of the daughter nucleus $(A-x)^*$ formed as a result of emission of one nucleon or a group of nucleons x:

$$\gamma+A\rightarrow x+(A-x)^*$$

$$\big\lfloor\!\xrightarrow{\gamma'}(A-x).$$

Despite certain complications in the analysis and interpretation of these γ spectra, it was found that the method makes it possible to obtain quantitative information about the partial photonucleon cross sections. The method is particularly informative if it is combined with direct spectrometry of the emitted particle.

There is now an accumulation of extensive factual material which spans a large number of nuclei of the $1d2s$ shell ($8\leqslant Z\leqslant 20$). These are the nuclei ^{17,18}O, ^{19}F, ^{23}Na, ^{24,25,26}Mg, ^{27}Al, ^{28,29,30}Si, ^{31}P, ^{32}S, ^{39}K, and ^{40}Ca. The total number of measured partial transitions for these nuclei is more than 300. All the information about the measured partial channels is available at the Center for Data of Photonuclear Experiments of the Nuclear Physics Institute of Moscow State University. It seems important to systematize this extensive and unique experimental material, thus elucidating the general characteristics of the decay of the giant dipole resonance in this region of nuclei. The analysis of this material is the subject of the present review, which is the first such systematization in the scientific literature.

We shall not describe the method of measurement of the secondary γ rays from deexcitation of the daughter nucleus produced as a result of the photonuclear reaction. The method is described in detail in Ref. 1, to which we refer the reader interested in this question.

2. REPRESENTATION OF THE EXPERIMENTAL DATA AND PRINCIPLES OF THEIR ANALYSIS

The main factual material on the partial photonucleon cross sections is presented in the form of tables. For each nucleus, the photoproton and photoneutron channels are given separately. An exception is the case of the nuclei ^{25,26}Mg, for which only the photoproton channel is given. The left sides of the tables give details about the occupied levels of the daughter nucleus $A-1$: the energy E_i, the spin and parity J^π, and the isospin T. Besides these quantum numbers, the tables give information about the spectroscopic factors C^2S_i extracted from pickup reactions of the type $(d,^3\mathrm{He})$, (p,d) on the initial nucleus A and the quantum numbers (n,l,j) that characterize the hole structure of the state i produced in the nucleus $A-1$.

The spectroscopic factors of the levels are given with the factor C^2 (C is the Clebsch–Gordan isospin coefficient). With this representation of the spectroscopic factor, it is easy to estimate the hole component of a level on the basis of the sum rule for this quantity. Thus, for $\Sigma_i C_i^2 S^{(p)}$, where the superscript indicates that we are dealing with proton pickup, we have the relation

$$\sum_i C^2S_i^{(p)}(nlj)=n^{(p)}(nlj), \tag{1}$$

where $n^{(p)}(nlj)$ is the number of protons in the subshell with quantum numbers (nlj), and $C^2=2T_i/(2T_i+1)$. The summation is over all states i of the final nucleus $A-1$. The quantity

$$\frac{C^2S_i^{(p)}(nlj)}{n^{(p)}(nlj)} \tag{2}$$

is the probability that the considered state of the nucleus $A-1$ is a proton hole in the corresponding subshell relative to the ground state of the nucleus A.

In the experiments, one can see only hole states corresponding to the outer shells, $1d_{5/2}$, $1d_{3/2}$, $2s_{1/2}$, and the inner $1p$ shell: $1p_{1/2}$ and $1p_{3/2}$. In the majority of cases, the spectroscopic factors are strongly fragmented over a rather broad energy region even for states corresponding to a hole in an outer shell. The $1p_{3/2}$ hole is particularly strongly fragmented. In a number of cases, there are practically no traces of it.

In the majority of the experiments, shells higher than $1d2s$ are not observed, and therefore the following analysis of the cross sections is based on the assumption that the

 1063-7796/95/040367-27$10.00

TABLE I. Integrated cross sections of $^{17}O(\gamma,p_i)^{16}N$ reactions extracted from the $(\gamma,p\gamma')$ experiment of Ref. 3 and characteristics of occupied ^{16}N levels (Refs. 6 and 7). E_γ^m=28 MeV.

	Characteristics of ^{16}N levels (T=1)				
i	E_i, MeV	J^π	nlj	C^2S_i	$\sigma^{int}(\gamma,p_i)$, MeV·mb
0	0	2^-	$1p_{1/2}$	0.94	17–19
2	0.298	3^-	$1p_{1/2}$	1.33	
1	0.120	0^-	—		2.0–2.5
3	0.397	1^-	—		
	$\sigma^{int}(\gamma, p)$				21±2 (Ref. 3)

TABLE II. Integrated cross sections of $^{17}O(\gamma, n_i)^{16}O$ reactions extracted from the $(\gamma, n\gamma')$ experiment of Ref. 3 and characteristics of occupied ^{16}O levels (Refs. 6 and 7). E_γ^m=28 MeV.

	Characteristics of ^{16}O levels (T=0)				
i	E_i, MeV	J^π	nlj	C^2S_i	$\sigma^{int}(\gamma,n_i)$, MeV·mb
0	0	0^+	$1d_{5/2}$	0.74	17–20 (Ref. 8)
1	6.05	0^+		—	<0.2
2	6.13	3^-	$1p_{1/2}$	0.46	3
3	6.92	2^+		—	<0.2
4	7.12	1^-		—	<0.2
5	8.89	2^-	$1p_{1/2}$	0.33	—
	$\sigma^{int}(\gamma, n)$				80–85 (Ref. 9)

TABLE III. Integrated cross sections of the $^{18}O(\gamma, p_i)^{17}N$ reaction from the $(\gamma, p\gamma')$ experiment of Ref. 4 and characteristics of the occupied ^{17}O levels.[6]

	Characteristics of ^{17}N levels (T=3/2)				$\sigma^{int}(\gamma,p_i)$, MeV·mb	
i	E_i, MeV	J^π	nlj	C^2S_i	E_γ^m=23.5 MeV	E_γ^m=28 MeV
0	0	$1/2^-$	$1p_{1/2}$	2.02	≤10	≤21
1	1.37	$3/2^-$	$1p_{3/2}$	0.38	0.31	2.01
2	1.85	$1/2^+$	$2s_{1/2}$	0.41	0.28	0.88
3	1.91	$5/2^-$		—	0.16	0.86
4	2.53	$5/2^+$	$1d_{5/2}$	0.53	—	—
6	3.20	$3/2^-$	$1p_{3/2}$	0.05	—	—
10	4.01	$3/2^-$	$1p_{3/2}$	0.04	—	—
11	4.21	$5/2^+$		—	0.31	0.88
		$\sigma^{int}(\gamma, p_i)$			25–26 (Ref. 5, E_γ^m=28 MeV)	

TABLE IV. Integrated cross sections of the $^{18}O(\gamma, n_i)^{17}O$ reaction from the $(\gamma, n\gamma')$ experiment of Ref. 4 and characteristics of the occupied ^{17}O levels.[6]

	Characteristics of ^{17}O levels (T=1/2)				$\sigma^{int}(\gamma, n_i)$, MeV·mb	
i	E_i, MeV	J^π	nlj	C^2S_i	E_γ^m=23.5 MeV	E_γ^m=28.0 MeV
0	0	$5/2^+$	$1d_{5/2}$	1.53	21 (Refs. 10 and 11)	24–26 (Refs. 10 and 11)
1	0.87	$1/2^+$	$2s_{1/2}$	0.21	6.01	6.71
2	3.06	1/2	$1p_{1/2}$	1.08	5.18	8.69
3	3.84	5/2		—	0.77	1.17
		$\sigma^{int}(\gamma, n_i)$			≅84 (Ref. 5, E_γ^m=28 MeV)	

nucleons occupy only the listed shells and, of course, $1s$. Thus, the configuration structure of the ground state of the initial nucleus is represented in the form

$$1s^4 1p^{12} 2s^{n_{1/2}}_{1/2} 1d^{n_{5/2}}_{5/2} 1d^{n_{3/2}}_{3/2}.$$

In accordance with this, the dipole resonance is formed from transitions of nucleons from an outer shell (group A) to an neighboring completely free shell,

$$(1d2s) \rightarrow (1f2p),$$

and from a deep closed shell (group B) to a partly filled shell,

$$1p \rightarrow (1d2s).$$

However, it should be borne in mind that calculations indicate that shells higher than $1d$ and $2s$ are also represented in the ground state of the initial nucleus A. Quantitative experimental data confirming occupation of higher orbits are available for ^{40}Ca (presence of magnetic dipole transitions) and ^{18}O (nonzero values of the proton spectroscopic factors to the levels $i=2$ and 4 of the ^{17}N nucleus). The corresponding spectroscopic factors will be given in the following section (Table III), in which we discuss the photodisintegration of the oxygen isotopes. Since in other nuclei direct quantitative information about high orbits is absent, they will not be taken into account in the present analysis.

The right-hand sides of the tables give the partial photonucleon cross sections, which are integrated over the region of the dipole resonance and are extracted from joint analysis of data on spectrometry of the nucleons and on the $(\gamma,x\gamma')$ reaction,

$$\sigma^{\text{int}}(\gamma,N_i)=\int_0^{E^m_\gamma}\sigma(\gamma,N_i)dE, \tag{3}$$

where E^m_γ is the upper limit of the γ-ray spectrum, i is the serial number of the occupied level in the nucleus $A-1$, and N characterizes the species of emitted nucleon (neutron or proton). If this quantity is obtained from both deexcitation experiments and nucleon spectrometry, both sets of data are given. At the bottom of the tables, we give the integrated photonucleon cross sections obtained in experiments without separation of the partial channels.

The levels of the final nucleus $A-1$ are occupied both by the semidirect mechanism and by the pre-equilibrium and equilibrium mechanisms. In the semidirect mechanism, the nucleon is emitted as a result of formation of a particle–hole state. Pre-equilibrium decay occurs after a particle–hole state has become more complicated. The cross section for occupation of each level in the final nucleus due to the semidirect mechanism can be estimated for self-conjugate nuclei on the basis of the relation

$$\sigma_{s\ \text{dir}}(\gamma,N_i(\beta))=\sigma_{\text{exp}}(\gamma,N_{\text{base}})\frac{\Gamma^\uparrow_i(N(\beta))}{\Gamma^\uparrow(N_{\text{base}}(\beta))}, \tag{4}$$

where $\sigma_{\text{exp}}(\gamma,N_{\text{base}})$ is the cross section of the partial photonucleon channel that is assumed to be due exclusively to the semidirect mechanism. We shall call it the base cross section. There must be one base cross section for each hole β. We shall regard the cross sections of transitions to the lowest states of the final nucleus $A-1$ with maximum weight of the corresponding hole component as base cross sections. Such an assumption is confirmed by theoretical analysis of the photoproton channel to the ground state of the final nucleus in the case of ^{28}Si, ^{32}S, and ^{40}Ca photodisintegration. In the tables, these base cross sections will be identified by an asterisk.

In Eq. (4), $\Gamma^\uparrow(N_i(\beta))$ is the resonance partial width associated with the semidirect emission of a nucleon that results in occupation of state i of the nucleus $A-1$ with respect to the hole component β, and $\Gamma^\uparrow(N_{\text{base}}(\beta))$ is the resonance partial width associated with decay through the hole channel β to the base level N_{base} in the nucleus $A-1$. Thus, for the base levels $\sigma_{s\ \text{dir}}(\gamma,N_i) = \sigma_{\text{exp}}(\gamma,N_i)$, while for the remaining levels $\sigma_{s\ \text{dir}}(\gamma,N_i) \leqslant \sigma_{\text{exp}}(\gamma,N_i)$.

The total width Γ of the resonance is equal to the sum of the partial widths of the semidirect transitions, $\Sigma_i\Gamma^\uparrow(N_i)$, and the width $\Gamma^\downarrow$ associated with the spread of the states over more complicated states:

$$\Gamma=\sum_i \Gamma^\uparrow(N_i)+\Gamma^\downarrow. \tag{5}$$

The ratio of the widths of the semidirect processes, which occurs in the expression (4), was calculated using the relations obtained from R-matrix theory and the shell model in the version with bound states (bound shell model). The corresponding relations were discussed in detail in the review of Ref. 1. Here we give only the final expressions used to make the calculations:

$$\frac{\Gamma^\uparrow(N_i(\beta))}{\Gamma^\uparrow(N_{\text{base}}(\beta))}=\frac{S(\varepsilon_i(\beta))}{S(\varepsilon_{\text{base}}(\beta))}\sqrt{\frac{\varepsilon_i}{\varepsilon_{\text{base}}}}\frac{P_l(\varepsilon_i)}{P_l(\varepsilon_{\text{base}})}. \tag{6}$$

Here $S(\varepsilon_i(\beta))$ is the spectroscopic factor obtained from the reaction of nucleon pickup from the ground state of the initial nucleus A with production of the nucleus $A-1$ in state i, ε_i is the energy of the nucleon emitted on decay of the state formed as a result of photoabsorption, $P_l(\varepsilon)$ is the penetrability of the barrier that the nucleon must overcome in order to be in the continuous spectrum, and l is the angular momentum carried away by the nucleon. The values of the spectroscopic factors and the quantum numbers of the hole components of the levels are given in the same tables in which the cross sections of the partial transitions are given.

Experimental data on partial neutron channels are much sparser than for the proton channels. To get a picture of them, we used a procedure for conversion to them from the proton cross sections. In even–even self-conjugate nuclei, the conversion was done in accordance with

$$\frac{\sigma(\gamma,n_i)}{\sigma(\gamma,p_i)}=\frac{\sqrt{\varepsilon_n}P_{l(n)}(\varepsilon_n)}{\sqrt{\varepsilon_p}P_{l(p)}(\varepsilon_p)}, \tag{7}$$

where the index n is for a neutron, and p for a proton, and $P_{l(n)}$ and $P_{l(p)}$ are the barrier penetrabilities for the neutron and proton, respectively. In a number of cases, this relation is used to estimate the photoproton cross section from the photoneutron cross sections.

In non-self-conjugate nuclei, the giant resonance has two isospin branches: $T_> = T_z + 1$ and $T_< = T_z$. The excitation

and decay schemes of both branches with proton and neutron emission are shown in Fig. 1. The figure also shows the relationships between these branches, which are determined by the Clebsch–Gordan coefficients.

The partial cross section associated with the semidirect component for a non-self-adjoint nucleus is determined by the expression

$$\frac{\sigma_{s\ \mathrm{dir}}(\gamma,N_i)}{\sigma_{\mathrm{exp}}(\gamma,N_{\mathrm{base}})} = \begin{cases} \dfrac{\sigma_<\Gamma^{\uparrow}_<(N_i)+a\sigma_>\Gamma^{\uparrow}_>(N_i)}{\sigma_<\Gamma^{\uparrow}_<(N_{\mathrm{base}})+a\sigma_>\Gamma^{\uparrow}_>(N_{\mathrm{base}})}, & \text{for branch of decay to levels with } T_i=T_z+1/2, \\ \Gamma^{\uparrow}_>(N_i)/\Gamma^{\uparrow}_<(N_{\mathrm{base}}), & \text{for } T_i=T_z-1/2. \end{cases} \quad (8)$$

Here

$$a=\Gamma_</\Gamma_>. \quad (9)$$

This ratio is a parameter that was varied to obtain the best description of the experimental data.

It is assumed that the width $\Gamma^{\uparrow}(N_i)$ is due to emission of nucleons with angular momentum $l=1$ and 3 (dipole transition from the d shell leads to transition of a nucleon to the $2p$ or f shell with subsequent nucleon emission). The ratio of the widths with fixed angular momentum was also a parameter used to fit the results:

$$\Gamma^{\uparrow}_<(N_i)=b_<\Gamma^{\uparrow}_<(l=3)+(1-b_<)\Gamma^{\uparrow}_<(l=1), \quad (10a)$$

$$\Gamma^{\uparrow}_>(N_i)=b_>\Gamma^{\uparrow}_>(l=3)+(1-b_>)\Gamma^{\uparrow}_>(l=1). \quad (10b)$$

The ratio of the cross sections $\sigma_<$ and $\sigma_>$ was determined from the relation[2]

$$\frac{\int(\sigma_>/E)dE}{\int(\sigma_</E)dE}=\frac{1}{T_z}\left(\frac{1-1.5T_zA^{-2/3}}{1+1.5A^{-2/3}}\right). \quad (11)$$

To make the calculations for a non-self-conjugate nucleus, the resonance was represented in the form of two states with $T_>$ and $T_<$ that take up the complete cross section. These states were ascribed energies corresponding to the centroids of the corresponding isospin components: $E_<$ and $E_>$. The semidirect components of the partial cross sections, integrated over the resonance, were calculated in accordance with the expression (8) with replacement on the left-hand side of $\sigma_{s\ \mathrm{dir}}(\gamma,N_i)$ and $\sigma_{\mathrm{exp}}(\gamma,N_{\mathrm{base}})$ by $\sigma^{\mathrm{int}}_{s\ \mathrm{dir}}(\gamma,N_i)$ and $\sigma^{\mathrm{int}}_{\mathrm{exp}}(\gamma,N_{\mathrm{base}})$, respectively.

For transitions to states associated with a $1p$ hole, the semidirect components of the cross sections were estimated on the basis of the principles described above only for the subshell $1p_{1/2}$, which has energy corresponding to the region of the $1d2s$ levels and, as a rule, is concentrated in 1–3 states of the final nucleus. For ^{17,18}O, the subshell $1p_{1/2}$ is essentially an outer shell. If the spectroscopic strength of the $1p_{1/2}$ hole is concentrated in one state (^{24}Mg, ^{28}Si), the occupation of this state (which could be regarded as a "pure" hole) was assumed to be entirely due to semidirect decay. It was found that the $1p_{1/2}$ shell increased the fraction of the semidirect mechanism by not more than 25%. In all cases, only an upper bound for the semidirect cross section was given for the deep $1p_{3/2}$ hole. For nuclei more massive than ^{28}Si, the $1p$ shell could not be seen at all in the partial cross sections. Details of the estimate of the contribution of the $1p$ shell to the semidirect part of the photonucleon cross sections for each nucleus can be found in the section devoted to the given nucleus.

3. RESULTS OF MEASUREMENTS AND ANALYSIS OF PARTIAL CROSS SECTIONS

3.1. The oxygen isotopes ^{17}O and ^{18}O

For the ^{17}O nucleus, there is one $(\gamma,x\gamma')$ experiment.[3] Its results for the nucleon channels $(x=p,n)$ are given together with the spectroscopic information in Tables I and II.

The photoproton cross section is mainly formed by transitions to the ground and the second excited state of the final nucleus ^{16}N; these are $p_{1/2}$ hole states. Their fraction is 80–95% of the total intensity of the proton channel. These transitions can be regarded as semidirect. The hole in the $p_{3/2}$ shell did not appear in the photoproton channel, since the corresponding levels in the ^{16}N nucleus are high.

In the photoneutron channel, the partial cross section associated with occupation of the ^{16}O ground state is found to be large. This corresponded to 20–25% of the intensity of the photoneutron channel. This channel is formed by the decay of a pygmy resonance—the low-energy branch of the dipole resonance due to transition of the only neutron in the valence $d_{5/2}$ shell to a higher shell as a result of absorption of a γ ray with subsequent emission to the continuous spectrum. It is natural to associate this partial cross section with the semidirect decay branch.

The remaining ^{16}O levels are weakly occupied, although there are among them two with fairly large spectroscopic factors. However, all these levels have isospin $T_i=0$. The main branch of the dipole resonance of the ^{17}O nucleus, for which the isospin takes the value $T=T_>=3/2$, cannot decay to these states of the ^{16}O nucleus. Decay of the $T_>$ branch of the resonance through the neutron channel must lead to occupation of levels of the ^{16}O nucleus with isospin $T=1$, which are isobar analogs of low-lying levels of the ^{16}N nucleus. They lie high in the continuous spectrum ($E^*\geqslant 12$ MeV) and cannot be identified by means of γ spectroscopy. The absence of information on the occupation of high-lying hole states of ^{16}O makes it possible to estimate only the lower limit of the contribution of the semidirect processes to the photoneutron channel. The limit is determined by $\sigma^{\mathrm{int}}(\gamma,n_0)$ and is about 20%.

For the ^{18}O nucleus too, a single $(\gamma,x\gamma')$ experiment has been made.[4] Its results for the nucleon channels $(x=p,n)$ are given together with the spectrometric information in Tables III and IV. The estimate of $\sigma^{\mathrm{int}}(\gamma,p_0)$ was obtained by subtracting from the integrated cross section of the photoproton reaction[5] (given in the final row of Table III) the total integrated cross section of the $(\gamma,p_{i>0})$ reactions.[4]

As we already noted in Sec. 1, in the ground state of ^{18}O there is not only the ground configuration $1s^41p^{12}(1d2s)^2$ but also the configuration $1s^41p^{10}(1d2s)^4$. Occupation of these levels in the photoproton reaction can occur both by

the semidirect mechanism through the second configuration and by inelastic rescattering of a particle by a hole formed by photoabsorption by the ground configuration. A theoretical investigation of the role of both mechanisms is interesting.

In contrast to ^{17}O, part of the strength of the proton $p_{3/2}$ hole in ^{18}O corresponds to a low-lying level of ^{17}N. However, the cross section of the partial photoproton channel for this level was found to be small.

Assuming that only level $i=0$ of the ^{17}N nucleus is occupied as a result of the semidirect process of decay of the giant dipole resonance (GDR), we find that its probability in the proton channel is $\leqslant 0.8$.

According to Ref. 5, the integrated photoneutron cross sections are

$$\int_0^{23} \sigma(\gamma,n+\gamma,np)dE_\gamma \simeq 59 \text{ MeV}\cdot\text{mb}$$

and

$$\int_0^{28} \sigma(\gamma,n+\gamma,np)dE_\gamma \simeq 84 \text{ MeV}\cdot\text{mb}.$$

Bearing in mind that on account of the high threshold (around 22 MeV) the cross section of the (γ,np) reaction is small, the measured cross section must be attributed to the (γ,n) reaction.

As in the case of the ^{17}O nucleus, the decay of the $T_>$ branch of the resonance in ^{18}O through the neutron channel must lead to occupation of levels of the daughter nucleus in the continuous spectrum. Therefore, it cannot be identified in the $(\gamma,x\gamma')$ experiment. As follows from the data of Ref. 5, the partial photoneutron transitions observed in the experiment of Ref. 4 exhaust only about 60% of the integrated cross section of the (γ,n) reaction.

The ground state and the first excited level of ^{17}O are neutron hole states of valence nucleons (in the subshells $1d_{5/2}$ and $2s_{1/2}$, respectively) with respect to the ground state of ^{18}O. The occupation of these levels is due to the decay of a pygmy resonance, i.e., a resonance formed by excitation of two outer neutrons. The second excited state is a $1p_{1/2}$ hole and is occupied in the photoneutron reaction by decay of the main branch of the dipole resonance in this nucleus, i.e., as a result of excitation of nucleons of an inner shell. The total cross sections of the (γ,n_0), (γ,n_1), and (γ,n_2) reactions, divided by $\sigma^{\text{int}}(\gamma,n)$, give lower bounds for the probabilities of semidirect processes in the photoneutron channel. With allowance for what we have said, the probability of semidirect processes in the neutron decay channel of the giant dipole resonance of the ^{18}O nucleus is not less than 0.55 ($E_\gamma^m=23.5$ MeV) and 0.47 ($E_\gamma^m=28$ MeV).

The data of Table IV make it possible to estimate the probabilities of the dipole transitions $1p\rightarrow 1d2s$ (group B) and $1d2s\rightarrow 1f2p$ (group A) in the formation of the GDR of the ^{18}O nucleus. Ascribing to group A the partial transitions that lead to occupation of positive-parity levels of the final ^{17}O nucleus, we find that their probability in the photoneutron channel is not less than 0.46 ($E_\gamma^m=23.5$ MeV) and 0.37 ($E_\gamma^m=28.0$ MeV). In the photoproton channel, the corresponding probability is in the interval 0.1–0.9 as a result of the large uncertainty in the data.

3.2. The ^{19}F nucleus

For the ^{19}F nucleus, two $(\gamma,x\gamma')$ experiments were made.[12,13] Tables V and VI give the results of the later and more complete experiment of Ref. 13. In addition, these tables give data from Refs. 14 and 15, in which the energy dependences of the cross sections of the (γ,p_i) and (γ,n_i) reactions were determined by photonucleon spectrometry. In the case of the photoneutron channel,[15] these data are restricted to the (γ,n_0) and (γ,n_1) reactions, which were investigated only up to $E_\gamma=19$ MeV. For the photoproton channel,[14] data on $\sigma(\gamma,p_i)$ were obtained up to $E_\gamma=25$–26 MeV and were extrapolated by us up to $E_\gamma=30$ MeV.

Comparison of the data of Refs. 13 and 14 (Table V) shows that in the $(\gamma,p\gamma')$ experiment it was not possible to identify transitions to levels with $E_i>5$ MeV of the ^{18}O nucleus, the intensity of which, according to Ref. 14, is very high. Among these levels, there are both $p_{1/2}$ and $p_{3/2}$ hole states. A fairly large fraction of the decay of the dipole state formed by excitation of a $1p$ nucleon must be to such levels.

In the final ^{18}F nucleus, the levels with isospin $T_i=1$ are low, and some of them are in a bound state. This opens up the possibility of detecting γ rays from decay of the $T_>$ branch of the resonance through the neutron channel. In the experiments, it was possible to identify transitions to such levels. They were $i=2$, 8, and 19.

The results of the estimates of the probability of semidirect decay in the different partial channels are given in the right-hand columns of Tables V and VI. In the estimates, we took into account the isospin and configuration splitting of the GDR of the ^{19}F nucleus in accordance with the data of Refs. 2 and 16–18. For $E1$ transitions from the outer $(1d2s)$ shell, we took the values $E(T_<)=18$ MeV and $E(T_>)=22.7$ MeV. For $\sigma_<$ and $\sigma_>$, we used the values 0.36 and 0.64 of Ref. 2. The ratio $a=\Gamma_</\Gamma_>$ was found to be 0.8. For the coefficients $b_<$ and $b_>$, which determine the degree of mixing with respect to the orbital angular momentum l of the emitted photonucleons in the semidirect decay of the $T_<$ and $T_>$ branches of the GDR, we obtained the values $b_<\simeq 0.70$–0.75 and $b_>\simeq 0.95$–1.0. This corresponds to the case when the semidirect decay of the $T_<$ branch of the GDR resonance occurs with probability 0.25–0.30 due to emission of photonucleons with $l=1$ and with probability 0.70–0.75 due to emission of photonucleons with $l=3$. It was found that the semidirect decay of the $T_>$ branch occurs almost exclusively through emission of photonucleons with $l=3$. It follows from the fact that the levels of the ^{18}F nucleus with zero isospin are occupied exclusively by decay of the $T_<$ branch of the GDR resonance that the production of the ^{18}F nucleus in states with $T=0$ must be accompanied by appreciable emission of neutrons with $l=1$.

For $E1$ transitions from the $1p$ shell in the photoproton channel, only an upper bound was estimated. With allowance for it, the integrated cross section of the semidirect processes in the photoproton channel was found to be

TABLE V. Integrated cross sections of the $^{19}F(\gamma, p_i)^{18}O$ reaction,[13,14] their semidirect components $\sigma^{int}_{s\,dir}$, and characteristics of the occupied ^{18}O levels (Refs. 20 and 21). $E^m_\gamma = 30$ MeV.

	Characteristics of ^{18}O levels ($T=1$)				$\sigma^{int}(\gamma, p_i)$, MeV·mb		$\sigma^{int}_{s\,dir}(\gamma,p_i)$, MeV·mb
i	E_i, MeV	J^π	nlj	C^2S_i	$(\gamma, p\gamma')$ Ref. 13	(γ, p_i) Ref. 14	
0	0	0^+	$2s_{1/2}$	0.38	—	11*	11
1	1.98	2^+	$1d_{5/2}$	0.53	20	12*	12
2	3.55	4^+	$1g_{9/2}$	0.04	<1.3		
3	3.64	0^+	$2s_{1/2}$	0.05±0.02	5.0±2.5	5	1.3–1.4
4	3.92	2^+	$1d_{5/2}$	0.02±0.01	2.5±1.25		0.3–0.4
5	4.46	1^-	$1p_{1/2}$	1.31	7.5±2.5	18–20	≤11
7	5.26	2^+	$1d_{5/2}$	0.32±0.1	—	11	2.5–4.0
8	5.34	0^+	$2s_{1/2}$	0.15±0.06			2.9–3.2
11	6.20	1^-	$1p_{3/2}$	0.70	—	≤14	<14
12	6.35	(2^-)					
14	6.88	0^-	$1p_{1/2}$	1.03	—	≤5*	≤5
16	7.62	1^-	$1p_{3/2}$	0.42	—	≤40	<40
17	7.77	2^-					
44	11.14			0.65			
48–49	11.75	$(0,1,2)^-$	$1p_{3/2}$	0.72	—	≤70	<70
51	12.25			0.89			
		$\sigma^{int}(\gamma,p)$			120–130 (Refs. 14 and 19)		
		$\sigma^{int}(\gamma,p+\gamma,np)$			160–170 (Ref. 14)		

$\Sigma_i \sigma^{int}_{s\,dir}(\gamma,p_i) = 30-100$ MeV·mb, corresponding to a probability of semidirect decay in the (γ,p) channel equal to 0.23–0.83.

For the photoproton channel, we used two different (a and b) base cross sections in the calculation of $\sigma^{int}_{s\,dir}(\gamma,n_i)$ corresponding to occupation of levels containing some of the

TABLE VI. Integrated cross sections of the $^{19}F(\gamma, n_i)^{18}F$ reaction,[13,15] their semidirect components $\sigma^{int}_{s\,dir}$, and characteristics of the occupied ^{18}F levels (Ref. 20). $E^m_\gamma = 30$ MeV.

	Characteristics of ^{18}F levels				$\sigma^{int}(\gamma, n_i)$, MeV·mb		$\sigma^{int}_{s\,dir}(\gamma, p_i)$, MeV·mb	
i	E_i, MeV	$J^\pi T$	nlj	C_i^2S	$(\gamma, n\gamma')$ Ref. 13	(γ, n) Ref. 15	a	b
0	0	1^+0	$2s_{1/2}$	0.65		>9	15*	55
1	0.94	3^+0	$1d_{5/2}$	1.47	12.5*±2.5	>11	12.5	
2	1.04	0^+1	$2s_{1/2}$	0.27	11.3*±2.5		1.8	11
3	1.08	0^-0	$1p_{1/2}$	0.38	2.5*±1.2		2.5	
5	1.70	1^+0	$2s_{1/2}$	0.07	<0.6		1.3	6.5
6	2.10	2^-0	$1p$	(0.03)	<1.3		—	
7	2.52	2^+0	$1d$	≅0	<0.5		—	
8	3.06	2^+1	$1d_{5/2}$	0.74	3.8±1.9		0.3–1.4	
9	3.13	1^-0	$1p_{(1/2)}$	1.04	3.8±1.3		5.2	
11	3.72		$2s_{1/2}$	0.015			0.15	1.3
			$1d_{5/2}$	0.22			0.4–1.2	
							0.8–2.6	
13	3.84		$1d_{(5/2)}$	0.5				
16	4.36	1^+0	$2s_{1/2}$	0.04			0.34	2.6
			$1d_{5/2}$	0.13			0.13–0.6	
19	4.75	0^+1	$2s_{1/2}$	0.03	0.88±0.25		0.09	0.89
			$1d_{5/2}$	0.08			0.02–0.09	
20	4.86	1^-0	$1p$	(0.11)			<0.2	
25	5.61	$1^-(0+1)$	$1p$	(0.82)			<1.6	
26	5.67	$1^-(0+1)$	$1p$	(0.44)			<0.9	
		$\sigma^{int}(\gamma,n)$				70–95 (Refs. 17 and 19)		
		$\sigma^{int}(\gamma,n+\gamma,pn+\gamma,2n)$				120–130 (Refs. 17 and 19)		

spectroscopic strength of the $2s_{1/2}$ hole. In case (b), the cross section for occupation of the level with $i=2$ was taken as the base. In this case we obtain for $\sigma^{\rm int}_{s\ {\rm dir}}(\gamma,n_0)$, and therefore for $\sigma^{\rm int}(\gamma,n_0)$, a rather large value: 55 MeV·mb. At the same time, it was found that $\Sigma_i\sigma^{\rm int}_{s\ {\rm dir}}(\gamma,n_i)$ $=100-107$ MeV·mb. With allowance for the fact that $\int_0^{30}\sigma(\gamma,n+\gamma,pn+\gamma,2n)dE_\gamma=120-130$ MeV·mb (see Ref. 19 and Table 24 in Ref. 17) and that the total contribution of the (γ,pn) and $(\gamma,2n)$ reactions to this quantity is 35–50 MeV·mb (Ref. 19), we find that the probability of semidirect processes in the (γ,n) channel of the ^{19}F nucleus is close to unity. In the total photoneutron reaction [i.e., with allowance for the contribution of the (γ,pn) and $(\gamma,2n)$ channels], this probability is 0.77–0.89.

Case (a) envisages the possibility that $\sigma^{\rm int}(\gamma,n_0)$ is much smaller than 55 MeV·mb. Rather arbitrarily, the value $\sigma^{\rm int}(\gamma,n_0)=15$ MeV·mb was chosen, and this cross section was taken as the base. In this version, the values of $\sigma^{\rm int}_{s\ {\rm dir}}(\gamma,n_i)$ for levels containing an admixture of the $2s_{1/2}$ hole are much smaller than in case (b). At the same time, we obtain $\Sigma_i\sigma^{\rm int}_{s\ {\rm dir}}(\gamma,n_i)$ = 41–48 MeV·mb, and the probability of the semidirect processes in the (γ,n) channel is found to be only 0.46–0.64. This is natural, since some of the semidirect decay of the $T_>$ branch through the neutron channel takes place to levels of the daughter nucleus in the continuous spectrum. As we shall see in what follows, case (b) fits much better into the systematization of the data on the semidirect decay of nuclei of the $1d2s$ shell than case (a). Combining the estimates of both possibilities, we find that the probability of the semidirect mechanism in the (γ,n) channel is $\geqslant$0.46. Note that for neutron decays to high-lying levels of the ^{18}F nucleus, which have a $1p$-hole nature ($i=20$, 25, 26), only an upper limit for the semidirect decay was estimated.

The fraction of the transitions of group A was 0.3–0.9 in $\sigma^{\rm int}(\gamma,p)$ and 0.48–0.93 in $\sigma^{\rm int}(\gamma,n)$. In the total integrated photonucleon cross section, the fraction of transitions of group A was 0.32–0.89.

3.3. The ^{23}Na nucleus

For this nucleus, two $(\gamma,x\gamma')$ experiments were made,[22,23] and there was one experiment to measure the energy dependences of the cross sections of the (γ,p_i) reactions.[24] Data of the experiments of Refs. 23 and 24 are given in Tables VII and VIII.

Details of the calculation of the semidirect components of the GDR of the ^{23}Na nucleus are given in Ref. 25. We give the results of these calculations. For $E1$ transitions from the outer $(1d2s)$ shell, we took the values $E(T_<)=17$ MeV and $E(T_>)=21$ MeV, and for transitions from the inner $1p$ shell we took $E(T_<)=21$ MeV and $E(T_>)=25$ MeV. For $\sigma_<$ and $\sigma_>$, we used the values 0.35 and 0.65. The following values of the parameters a and b ensure the best description of the experimental data: $a=0.7-0.8$, $b_<=0.98$, $b_>=1.0$. Thus, the calculation indicates dominant emission of nucleons with $l=3$ in the $E1$ transitions $1d\rightarrow(1f2p)$.

For levels containing a hole admixture in the $1d_{5/2}$ subshell, either $\sigma(\gamma,p_1)$ or $\sigma(\gamma,n_6)$ was taken as the base cross section. The corresponding final states are isobar analogs. For the neutron channels, $\sigma(\gamma,n_6)$ was used as the base cross section. The uncertainty in $\sigma^{\rm int}_{s\ {\rm dir}}(\gamma,p_i)$ for $i=1$, 2, and 3 is due to the two choices mentioned above for the base cross section, and the lower bound for $\sigma^{\rm int}_{s\ {\rm dir}}(\gamma,p_{i=1,2,3})$ corresponds to the choice of $\sigma(\gamma,n_6)$ as base cross section, and the upper bound to $\sigma(\gamma,p_1)$.

The sum of the integrated partial cross sections of the (γ,p_i) reactions obtained in the $(\gamma,p\gamma')$ experiment with the addition of $\sigma^{\rm int}(\gamma,p_0)=4.0$ MeV·mb is 61 MeV·mb. This means that in approximately 60% of the cases the (γ,p) reaction leads to occupation of levels of the ^{22}Ne nucleus with $i>10$, about which information was not obtained in the $(\gamma,p\gamma')$ experiment.

The sum of the partial photoneutron cross sections is about 80 MeV·mb, indicating that the main channels through which the excited levels of the ^{22}Na nucleus are occupied have been revealed. The remaining (unrevealed) part of the neutron cross section is about 1/4 of this value and is associated with the neutron decay channel of the $T_>$ branch, which takes place to states in the continuous spectrum.

It follows from Tables VII and VIII that $\Sigma_i\sigma^{\rm int}_{s\ {\rm dir}}(\gamma,p_i)$ = 26–46 MeV·mb, while $\Sigma_i\sigma^{\rm int}_{s\ {\rm dir}}(\gamma,n_i)$ = 63–75 MeV·mb. From this we conclude that the probability of the semidirect processes in the (γ,p) channel of the ^{23}Na nucleus is 0.17–0.31, while in the (γ,n) channel it is 0.60–0.71. At the same time, the fraction of the semidirect processes in $\sigma^{\rm int}(\gamma,p+\gamma,n)$ is 0.34–0.47. A small fraction of semidirect protons is obtained because the occupation of the high-lying levels of the ^{22}Ne nucleus with $i>10$, including ones with an admixture of a hole in the $1p_{3/2}$ subshell, takes place through nonsemidirect processes. The semidirect protons from this subshell can somewhat increase the probability of the semidirect mechanism in the proton channel and in the total photonucleon cross section.

The semidirect decay of states of the GDR that are formed by $E1$ transitions of group A, $(1d2s)\rightarrow(1f2p)$, leads to occupation of levels of the final nuclei of positive parity. As follows from Tables VII and VIII, the fraction of such decays (i.e., the probability of excitation of $E1$ transitions of group A in the ^{23}Na nucleus) is 0.47–0.94 in the (γ,p) cross section and about 0.90 in the (γ,n) cross section.

3.4. The magnesium isotopes ^{25}Mg and ^{26}Mg

We discussed the partial cross sections in the ^{24}Mg nucleus in the previous review of Ref. 1, and therefore we shall not consider this question here. Data on the partial cross sections of the (γ,p_i) reaction were obtained for the magnesium isotopes $A=25$ and 26 in an $(\gamma,p\gamma')$ experiment.[27] In addition, data on the (γ,p_i) cross sections were extracted from the spectra of the protons in an $(e,e'p)$ experiment[28] for ^{25}Mg and in a (γ,p) experiment[29] for ^{26}Mg. Tables IX and X give the integrated partial photoproton cross sections taken from the listed studies of Refs. 27–29. The upper limits for the γ-ray energy in Ref. 27 were 28.7 MeV for ^{25}Mg and 30 MeV for ^{26}Mg. In Refs. 28 and 29, these limits were 28 and 27 MeV, respectively.

In ^{25}Mg and ^{26}Mg, the photoneutron channel is dominant. Its fraction corresponds to 60–70% of the integrated

photoabsorption cross section. However, at the present time there are no reliable data on the partial photoneutron cross sections of these nuclei, and this prevents us from using our procedure to extract the semidirect components of the cross section. Therefore, the following discussion will relate only to the photoproton channel.

Even the data of the $(\gamma,p\gamma')$ experiment for ^{25}Mg and ^{26}Mg are rather sparse, especially for ^{26}Mg. Many partial channels could not be identified (there is a dash in the corresponding column) because of methodological difficulties (small cross section, complicated chain of γ cascade transitions, strong background γ lines). In particular, there are no data on the occupation of individual levels with $E_i>3$ MeV. Without the data of the experiments of photon spectrometry,[28,29] the extraction of the semidirect components of the photoproton cross sections would be impossible.

Details of the procedure for extracting the semidirect components $\sigma(\gamma,p_i)$ of the ^{25,26}Mg nuclei are described in Ref. 30. The configuration splitting for the $E1$ transitions from the $1d2s$ and $1p$ shells was taken into account. Isospin splitting was taken into account only for $(1d2s)\rightarrow(1f2p)$ transitions. To simplify the calculations, the $1p\rightarrow(1d2s)$ branch was approximated by one state, i.e., its splitting into isospin components was not taken into account. Data on the energies of the dipole states used in the calculations are given in Table XI.

For $\sigma_<$ and $\sigma_>$, we used the values 0.39 and 0.61 for ^{25}Mg ($T_z=1/2$) and 0.58 and 0.42 for ^{26}Mg ($T_z=1$). The value of the constant a was varied in the interval 0.5–2.0. The variation of a in this interval had a weak effect on the results of the calculations.

In the analysis it was assumed that the known sum of the cross sections of the partial transitions to the levels $i=0$, 1, and 2 of the ^{25}Na nucleus is due solely to the ground state. For the partial cross sections for occupation of states containing an admixture of a hole in the $2s_{1/2}$ subshell, only upper bounds on the probability of semidirect decay could be obtained, since the probability of the semidirect processes in the corresponding base cross sections is unknown. For the partial cross sections for occupation of states of the final nucleus containing an admixture of a hole in the $1d_{3/2}$ subshell, the (γ,n_2) cross section was chosen in the case of ^{26}Mg. Its value was determined in Ref. 27 and is $\sigma^{\rm int}(\gamma,n_2)=4.0$ MeV·mb. It was assumed that this cross section is entirely formed by semidirect decays. The occupied level of the final nucleus ^{25}Mg has $J^\pi=3/2^+$ and contains an appreciable admixture of a hole in the $1d_{3/2}$ subshell.

For the channels of the ^{25}Mg(γ,p_i) reaction leading to occupation of a $1d_{3/2}$ hole, only upper bounds for the semidirect components of the cross sections were obtained. For the base cross section, the part of $\sigma^{\rm int}(\gamma,p_1+p_2)$ due to decay to a $1d_{3/2}$ hole was taken. Only an upper limit on this cross section, which is 6.0 MeV·mb (see Table IX), is known.

For the hole states in the $1p$ shell, the base cross sections were taken to be those for occupation of levels with excitation energies $E_i=3.93$ MeV, 4.52 MeV, and 5.24 MeV for the ^{24}Na nucleus and the cross section for occupation of the level $i=12$ of the ^{25}Na nucleus. In this last case, the value of the cross section was estimated from the experimentally obtained[29] distribution of the probability for occupation of different levels of the final nucleus in the ^{26}Mg$(\gamma,p)^{25}$Na reaction. Since in both isotopes the fraction of the semidirect decays in the base cross sections to the $1p$ levels is unknown, only an upper bound for the semidirect component was estimated.

The data of Tables IX and X make it possible to determine the probability of $E1$ transitions from the outer shell, $(1d2s)\rightarrow(1f2p)$, in the photoproton channel. For ^{25}Mg, such transitions lead, after proton emission, to occupation of positive-parity states of ^{24}Na containing an admixture of a proton hole in the $1d2s$ shell in the ground state of ^{25}Mg. As can be seen from Table IX, states with $i\leqslant12$ correspond to just such states. It follows from this that

$$\sum_{i=0}^{12}\sigma^{\rm int}(\gamma,p_i)=48\ \ \text{MeV}\cdot\text{mb},$$

and this is 0.53 of the integrated cross section of the photoproton reaction. This value is a lower bound for the probability of $(1d2s)\rightarrow(1f2p)$ transitions in the photoproton cross section of the ^{25}Mg nucleus.

The partial cross sections for occupation of ^{24}Na states in the interval 3.22 MeV$\leqslant E_i<$6.90 MeV contain in an unseparated form the cross sections for occupation of both positive- and negative-parity states. If it is assumed that the partial cross sections in this region are formed solely by occupation of positive-parity states, then for the probability of $(1d2s)\rightarrow(1f2p)$ transitions we obtain the upper bound 0.83.

The occupation of ^{24}Na levels with $E_i\geqslant6.90$ MeV is due almost entirely to decay of the branch of the GDR of the ^{25}Mg nucleus that is excited by $1p\rightarrow(1d2s)$ transitions. In particular, this is indicated by the fact that above this energy there are no levels containing an appreciable fraction of the spectroscopic strength corresponding to the $1d2s$ level. Indeed, the C^2S_i sum for the positive-parity levels in the region $0\leqslant E_i\leqslant4.94$ MeV is 3.95 in a sum rule of 4.0 (the total number of protons in the $1d2s$ shell of the ^{25}Mg nucleus). Thus, the probability of $(1d2s)\rightarrow(1f2p)$ transitions in the photoproton cross section of the ^{25}Mg nucleus is 0.53–0.83.

A similar study for ^{26}Mg leads to the estimate 0.56–0.63 for the probability of $(1d2s)\rightarrow(1f2p)$ transitions. The spread is due to the uncertainty in $\sigma^{\rm int}(\gamma,p_{12})\leqslant8.0$ MeV·mb (Ref. 30).

3.5. The silicon isotopes ^{28,29,30}Si

^{28}Si. For this nucleus, a single $(\gamma,x\gamma')$ experiment has been performed.[31] Its results are given in Tables XII and XIII. In addition, there have been several investigations of the energy dependences of the partial photoproton cross sections.[32–36] These studies were made using various methods: with bremsstrahlung photons,[32] monochromatic annihilation[36] and tagged[33] photons, monochromatic polarized photons obtained from scattering of a laser beam by an electron beam,[34] and also by the $(e,e'p)$ method.[35] There are also data of (p,γ_0) (Ref. 37) and (γ,n_0) (Ref. 38) experiments. The combined data of the most detailed investigations of $\sigma(\gamma,p_i)$ for $i=1-10$ (Refs. 33, 36, and 37) are given in the

TABLE VII. Integrated cross sections of the ^{23}Na(γ, p_i)^{22}Ne reaction[23,24] in MeV·mb, their semidirect components $\sigma^{\text{int}}_{s\,\text{dir}}$, and characteristics of the occupied ^{23}Ne levels.[26]

	Characteristics of ^{22}Ne levels ($T=1$)				$\sigma^{\text{int}}(\gamma, p_i)$, MeV·mb		
i	E_i, MeV	J^π	nlj	C^2S_i	(γ, $p\gamma'$) (Ref. 23) E^m_γ=32 MeV	(γ,p) (Ref. 24) E^m_γ=29.5 MeV	$\sigma^{\text{int}}_{s\,\text{dir}}(\gamma, p_i)$, MeV·mb
0	0	0^+	$1d_{3/2}$	0.08	—	4.0*	4.0
1	1.27	2^+	$1d_{5/2}$	1.13	20.7±3.8	23.5*	10–22
2	3.36	4^+	$1d_{5/2}$	0.41	9.2±1.9	21.6	1.9–3.8
3	4.46	2^+	$2s_{1/2}$	0.11	7.0±1.9		≤5.0
			$1d_{5/2}$	0.23			0.6–1.310
4	5.15	2^-	$1p_{1/2}$	1.73	9.4±3.8		
5	5.34	1^+		—	(1.0±0.4)	30.8	
6	5.37	2^+		—	3.5±1.3		
8	5.64	3^+		—	3.1±1.5		
10	6.12	2^+		—	2.8±1.5		
	$\bar{E}_i$=6.9 MeV			—		51	
	$\bar{E}_i$=8.9 MeV			—		27	
	$\bar{E}_i$=11.8 MeV			—		31	
	$\sigma^{\text{int}}(\gamma, p)$				150–155	(Ref. 23, E^m_γ=30 MeV)	

second column on the right of Table XII. The values of $\sigma^{\text{int}}(\gamma,p_i)$ given in this column were obtained by extrapolation of $\sigma(\gamma,p_i)$ obtained in Refs. 33, 36, and 37 to E_γ=28 MeV. In the studies of Refs. 33 and 36, $\sigma(\gamma,p_i)$ were not determined for $i>10$ (because of the restriction with respect to the excitation energy of the target nucleus). In Table XII, we give for $\sigma^{\text{int}}(\gamma,p_{i>10})$ the value 20 ± 6 MeV·mb, which was taken from the only experiment[32] in which this cross section was determined.

It should be noted that the data of the ($\gamma,p\gamma'$) experiment of Ref. 31 not only agree well with the data of the remaining studies represented in Table XII but in two cases

TABLE VIII. Integrated cross sections of the ^{23}Na(γ, n_i)^{22}Na reaction[23] in MeV·mb, their semidirect components $\sigma^{\text{int}}_{s\,\text{dir}}$, and characteristics of the occupied ^{22}Na levels.[26]

	Characteristics of ^{22}Na levels				$\sigma^{\text{int}}(\gamma, n_i)$, MeV·mb (Ref. 23)	$\sigma^{\text{int}}(\gamma, n_i)$, MeV·mb
i	E_i, MeV	$J^\pi T$	nlj	C^2S_i		
0	0	3^+0	$1d_{5/2}$	0.97	—	19.6
1	0.58	1^+0	$1d_{5/2}$	0.39	—	5.3
2(0)	0.66	0^+1	$1d_{3/2}$	0.04	—	5.0–7.5
3	0.89	4^+0	$1d_{5/2}$	0.94	9.6±2.5	10
4	1.53	5^+0		—	0.9±0.25	
6(1)	1.95	2^+1	$1d_{5/2}$	0.58	9.6±1.5*	10
7	1.96	3^+0	$1d_{5/2}$	0.58	2.1±0.6	2.1
8	2.21	1^-0	$1p_{1/2}$	0.53	2.5±1.0	2.9
9	2.57	2^-0	$1p_{1/2}$	0.41	3.0±0.75 *	2.6
11	3.06	2^+0	$1d_{5/2}$	0.07	1.8±0.9	0.05
14	3.94	1^+0	$2s_{1/2}$	0.07	1.13±0.25	≤1
15(2)	4.07	4^+1	$1d_{5/2}$	0.21	1.4±0.5	1.3
16	4.30	$(0^-)0$		—	2.3±1	
17	4.32	1^+0		—	1.0±0.5	
18	4.36	2^+0	$2s_{1/2}$	0.05	1.0±0.25	≤0.13
			$1d_{5/2}$	0.05		0.01
20	4.52	$7^+(5^+)0$		—	1.13±0.38	
21	4.58	2^-0	$1p_{1/2}$	0.67	1.8±0.8	2.5
23	4.71	5^+0		—	1.0±0.38	
27(3)	5.17	$(1.2)^+1$	$2s_{1/2}$	0.05	6.0±1.9*	≤6.3
			$1d_{5/2}$	0.11		0.25
	5.96	2 1	$1p_{1/2}$	0.87	-	1.3–3.8
			$\sigma^{\text{int}}(\gamma, n)$		105 (Ref. 23 (E^m_γ=30 MeV)	

[a]In brackets in the first column the number of the corresponding isobar-analog level of the ^{22}Ne nucleus is given.

TABLE IX. Integrated cross sections of the $^{25}Mg(\gamma,p_i)^{24}Na$ reaction, their semidirect components $\sigma^{int}_{s\ dir}$, and characteristics of the occupied ^{24}Na levels.[26]

Characteristics of ^{24}Ne levels ($T=1$)						$\sigma^{int}(\gamma, p_i)$, MeV·mb		
i	E_i, MeV (Ref. 28)	E_i, MeV (Ref. 26)	J^π	nlj	C^2S_i	$(\gamma, p\gamma')$ (Ref. 27)	(γ, p) (Ref. 28)	$\sigma^{int}_{s\ dir}(\gamma, p_i)$, MeV·mb
0	0	0	4^+	$1d_{5/2}$	1.37	—	11.8	11.8*
1	0.51	0.47	1^+	$1d_{5/2}$	0.24	—		1.6–1.7
2		0.56	2^+	$1d_{3/2}$	0.17	—		<6.0*
				$2s_{1/2}$	0.16	-	7.6	≤3.0
3		1.341	2^+			—		2.7–2.9
4		1.345	3^+	$1d_{5/2}$	0.58	6.09	12.2	
5	1.43	1.347	1^+			2.20		
6		1.51	$(3.5)^+$	$1d_{5/2}$	0.53	2.21		2.2–2.5
7	1.89	1.85	2^+	$1d_{5/2}$	0.04			0.15
8		1.89	3^+	$1d_{3/2}$	0.03	—	5.3	<0.6
				$2s_{1/2}$	0.07	3.72		≤1.1
9	2.53	2.51	3^+	$1d_{5/2}$	0.06			0.15
10		2.56	$(2,4)^+$	$1d_{3/2}$	0.11	1.25	5.1	<1.5
				$2s_{1/2}$	0.08	3.67		<1.0
11	2.91	2.91	3^+	$2s_{1/2}$	0.15	1.15	6.1	≤1.15*
12		2.98				—		
13		3.22	$(2.4)^+$	$1d_{5/2}$	0.08			0.11–0.14
14	4.0	3.37	2^-	$1p_{3/2}$	0.15		10.7	≤1.7
18		3.65	$(1-3)^+$	$1d_{5/2}$	0.11			0.08–0.14
		3.93		$1p_{1/2}$	1.18			≤10.5*
		4.94		$1d_{5/2}$	0.17		10.2	0.02–0.07
	5.0	4.52		$1p_{3/2}$	0.78			≤10.0*
		5.24		$1p_{3/2}$	0.40			
	6.0						6.7	0
	7.0	6.90		$1p_{3/2}$	0.29		4.1	2.7
		7.07		$1p_{3/2}$	0.52			
		8–13		$1p_{3/2}$	≤2.0		11.1	≤0.1
		$\sigma^{int}(\gamma,p+\gamma,pn)$ / $\sigma^{int}(\gamma,p)$				90±10 (Ref. 28) (E^m_γ=28 MeV) / 75±10 (Ref. 28)		

make them appreciably more accurate. Thus, according to Ref. 31, $\sigma(\gamma,p_{5+6})\simeq\sigma(\gamma,p_5)$ and $\sigma(\gamma,p_{8+9})\simeq\sigma(\gamma,p_9)$. In both cases, states of the ^{27}Al nucleus manifested in single-nucleon pickup are occupied.

There are significantly fewer data on $\sigma^{int}(\gamma,n_i)$. Here it is necessary to rely almost entirely on the $(\gamma,n\gamma')$ experiment of Ref. 31, augmented by the $\sigma^{int}(\gamma,n_0)$ data from Ref. 38. In Refs. 39 and 40, experimentally determined $\sigma(\gamma,p_i)$ values were used to calculate $\sigma(\gamma,n_i)$. The resulting values are given in the second column on the right in Table XII. Here it must be borne in mind that $\sigma(\gamma,n_{5+6})\simeq\sigma(\gamma,n_5)$ and $\sigma(\gamma,n_{8+9})\simeq\sigma(\gamma,n_9)$. The calculations of the photoneutron cross sections used the energy dependence of the cross section to the ground state $\sigma(\gamma,n_0)$ (Ref. 38), $\sigma^{int}(\gamma,n_i)$ from Ref. 31, and the energy dependence of the total photoneutron cross section (see, for example, Ref. 19), which was compared with $\Sigma_i\sigma(\gamma,n_i)$, where $\sigma(\gamma,n_i)$ were obtained by conversion from $\sigma(\gamma,p_i)$. It was found that agreement of the converted and experimental photoneutron cross sections is possible only under the following assumptions about the angular momentum of the emitted neutrons: In the region $E_\gamma\leqslant 19$ MeV, the neutrons have orbital angular momentum $l=1$; in the region $E_\gamma=19$–20.5 MeV, emission of neutrons with both $l=1$ and $l=3$ is possible, and the fraction of neutrons with $l=3$ increases with increasing E_γ; finally, for $E_\gamma\geqslant 20.5$ MeV, the emitted neutrons have predominantly $l=3$.

The total fraction of semidirect processes in $\sigma^{int}(\gamma,p)$ is 0.66–0.86, and in $\sigma^{int}(\gamma,n)$ it is close to 1 (0.93–0.96). In $\sigma^{int}(\gamma,p+\gamma,n)$, the probability of semidirect processes is 0.74–0.89.

Besides $\sigma(\gamma,p)$ and $\sigma(\gamma,n)$, a significant contribution to the photoabsorption cross section for the ^{28}Si nucleus is made by $\sigma(\gamma,\alpha)$ (Ref. 40). According to Ref. 33, $\sigma^{int}(\gamma,\alpha)\simeq 30$ MeV·mb, and this cross section is, in accordance with the conclusions of Ref. 41, formed mainly by statistical forms of decay of the GDR. Bearing in mind what we have said above, we find that the fraction of semidirect processes in the integrated photoabsorption cross section for the ^{28}Si nucleus up to 28 MeV can be estimated at the level 0.66–0.80.

The uncertainty in the values obtained for $\sigma^{int}_{s\ dir}(\gamma,x_i)$ is due to the uncertainty in the base cross sections and the uncertainty in the degree of mixing with respect to the orbital angular momentum of the emitted neutrons.

TABLE X. Integrated cross sections of the $^{26}Mg(\gamma,p_i)^{25}Na$ reaction, their semidirect components $\sigma^{int}_{s\,dir}$, and characteristics of the occupied ^{25}Na levels.[26]

	Characteristics of ^{25}Na levels ($T=3/2$)					$\sigma^{int}(\gamma,p_i)$, MeV·mb		
i	$\bar{E}_i$, MeV (Ref. 29)	E_i, MeV (Ref. 26)	J^π	nlj	C^2S_i	$(\gamma, p\gamma')$ (Ref. 27)	(γ, p) (Ref. 29)	$\sigma^{int}_{s\,dir}(\gamma, p_i)$ MeV·mb
0	0	0	$5/2^+$	$1d_{5/2}$	2.8	—	41.2	≅40*
1		0.9	$3/2^+$	$1d_{3/2}$	0.22	—		0.4–0.9
2		1.0	$1/2^+$	$2s_{1/2}$	0.35	<2.7		<2.7*
3	3	2.20	$3/2^+$	$1d_{3/2}$	0.12	—	26.8	0.1–0.2
5		2.79	$1/2^+$	$2s_{1/2}$	0.06	—		<0.3
6		2.91	$5/2^+$	$1d_{5/2}$	0.32	1.0		1.0–1.4
9		3.69	$(3/2,5/2)^+$	$(1d_{3/2},1d_{5/2})$	(0.08)	—		≤0.2
10		3.93	$1/2^+$	$2s_{1/2}$	(0.06)	—		<0.2
12		4.00	$(1/2,3/2)^-$	$(1p_{1/2},1p_{3/2})$	1.8	—		≤8.0*
14		4.29	$1/2^+$	$2s_{1/2}$	0.08	—		<0.2
21	6	5.19	$(1/2,3/2)^-$	$(1p_{1/2},1p_{3/2})$	0.7	—	39.2	≤2.7
27		5.69			0.18	—		≤0.7
31		6.01			0.08	—		≤0.3
34		6.55			0.22	—		≤0.7
35		6.75			<0.12	—		<0.2
39		7.60			0.3	—		≤0.7
41		8.05			<0.18	—		<0.2
		$\sigma^{int}(\gamma,p)$				107 (Ref. 29), (E^m_γ=27 MeV)		

The data of Tables XII and XIII make it possible to estimate the fraction of $(1d2s)\rightarrow(1f2p)$ transitions in the GDR of the ^{28}Si nucleus. The $(1d2s)\rightarrow(1f2p)$ transitions form practically all the partial photoneutron cross sections. An exception is $\sigma(\gamma,n_9)$. In the photoproton channel, the cross sections are $\sigma(\gamma,p_i)$ with $i=0$–8 and 10. The $1p\rightarrow(1d2s)$ transitions are manifested essentially only in the photoproton channel, and their fraction is 15–20% of $\sigma^{int}(\gamma,p)$. The fraction of $1p\rightarrow(1d2s)$ transitions in the integrated photonucleon cross section [including $\sigma^{int}(\gamma,n)$] is 11–14%.

The cross sections $\sigma^{int}(\gamma,p_9)$ and $\sigma^{int}(\gamma,n_9)$ can be taken as upper bounds on the semidirect cross sections corresponding to $1p_{1/2}\rightarrow(1d2s)$ transitions. The $1p_{3/2}\rightarrow(1d2s)$ transitions contribute only to $\sigma(\gamma,p_i)$ with $i\geq14$. The strong spreading of the $1p_{3/2}$ hole of the ^{28}Si nucleus over the states of the ^{27}Al nucleus and also the theoretical calculation of Ref. 42 indicate that the fraction of semidirect processes in the branch of the GDR of the ^{28}Si nucleus that is associated with excitation of the $1p_{3/2}$ subshell is small and can be ignored.

^{29}Si. Data of the only $(\gamma,x\gamma')$ experiment[43] for ^{29}Si, performed at E^m_γ=26 MeV, are given in Tables XIV and XV.

TABLE XI. Positions of centroids of the energies of dipole states (in mega-electron-volts) used in the procedure to extract the semidirect components of the GDR of the $^{25,26}Mg$ nuclei.

	$(1d2s)\rightarrow(1f2p)$		$1p\rightarrow(1d2s)$
Nucleus	$T_<$	$T_>$	Both isospin branches
^{25}Mg	18.0	21.6	23.6
^{26}Mg	20.0	24.6	24.6

For this nucleus, integrated cross sections of the $(\gamma,n+\gamma,np)$ and (γ,p) reactions[43,44] were also determined; up to E^m_γ=26 MeV, they were found to be 137±14 and 197–226 MeV·mb, respectively; according to the estimates, the contribution of $\sigma^{int}(\gamma,np)$ to the photoproton cross section does not exceed 10 MeV·mb. The cross sections of the (γ,p_0+p_1) and (γ,n_0) channels given in the tables were obtained by subtracting from $\sigma^{int}(\gamma,p)$ and $\sigma^{int}(\gamma,n)$ the total integrated cross sections for occupation of excited levels of ^{28}Al and ^{28}Si, respectively.

In Tables XIV and XV, all the $1d$ hole levels have been ascribed the $1d_{5/2}$ configuration. With allowance for the isospin splitting, we set $E(T_<)$=17.0 MeV, $E(T_>)$=20.1 MeV, $\sigma_<$=0.36, $\sigma_>$=0.64. For the $1d_{5/2}$ subshell, the calculation was made with two forms of base cross section: $\sigma^{int}(\gamma,p_0+p_1)$ and $\sigma^{int}(\gamma,n_1)$. The two possibilities gave practically the same results, confirming the proximity of $\sigma^{int}(\gamma,p_0+p_1)$ to the value 100 MeV·mb.

The range of possible values of $\sigma^{int}_{s\,dir}(\gamma,x_i)$ for the ^{28}Al and ^{28}Si levels containing an admixture of a $1d_{5/2}$ hole (see Tables XIV and XV) is due to the use of the two forms of base cross section. The largest value corresponds to the choice of the base cross section for occupation of the level with i=1 of the ^{28}Si nucleus (47.0 MeV·mb). The best description of the experimental data was obtained for the following values of the parameters a and b: a=0.8–0.9, $b_<$=0.7, $b_>$=1.0. We see that the semidirect decay of the GDR of the ^{29}Si nucleus with occupation of $1d^{-1}$ levels is accompanied by the predominant emission of nucleons with orbital angular momentum l=3 and ratio $\Gamma_</\Gamma_>$ not less than unity. The first of these facts indicates that the $1d\rightarrow(1f2p)$ transitions predominate over the $1d\rightarrow1f$ transitions.

The calculation of the probability of semidirect pro-

TABLE XII. Integrated cross sections of the $^{28}Si(\gamma,p_i)^{27}Al$ reaction (Refs. 31–33, 36, and 37), their semidirect components $\sigma^{int}_{s\,dir}$, and characteristics of the occupied states of the ^{27}Al nucleus (Ref. 26). $E^{m}_{\gamma}=28$ MeV.

Characteristics of ^{27}Al levels ($T=1/2$)					$\sigma^{int}(\gamma,p_i)$, MeV·mb		$\sigma^{int}_{s\,dir}(\gamma,p_i)$, MeV·mb
i	E_i, MeV	J^{π}	nlj	C^2S_i	(Ref. 31)	(Refs. 32, 33, 36, and 37)	
0	0	$5/2^+$	$1d_{5/2}$	3.2		60–65*	60–65
1	0.84	$1/2^+$	$2s_{1/2}$	0.7	35 ± 15	28–33*	28–33
2	1.01	$3/2^+$	$1d_{3/2}$	0.65	20 ± 6	11–15*	11–15
3	2.21	$7/2^+$	—	—	<2	2–3	0
4	2.73	$5/2^+$	$1d_{5/2}$	0.6	13 ± 2	7–10	3–7
5	2.98	$3/2^+$	$1d_{3/2}$	0.35	12±2	8–10	3–9
6	3.00	$9/2^+$	—	—	—		
7	3.68	$1/2^+$	$2s_{1/2}$	0.03	8 ± 2	4–6	0.06-0.07
8	3.96	$3/2^+$	$1d_{3/2}$	—	—	7–9	≤7–9
9	4.05	$1/2^-$	$1p_{1/2}$	1.8	9±2		
10	4.41	$5/2^+$	$1d_{5/2}$	0.38	—	1.5–2.0	≤0.2
14	5.16	$3/2^-$	$1p_{3/2}$	1.35	—		—
-						20±6	
-							
-							
		$\sigma^{int}(\gamma,p)$				150–175 (Refs. 32, 33, 36, and 37)	

cesses for the upper limit of integration 26 MeV gives for the photoproton and photoneutron channels the values 0.51–0.59 and 0.67–0.78, respectively.

All the observed partial transitions correspond to excitations of nucleons of the $1d2s$ shell, i.e., they correspond to $E1$ transitions of group A. This indicates that for ^{29}Si the contribution of the transitions of group B ($1p \rightarrow 1d2s$) up to $E_\gamma=26$ MeV is small.

^{30}Si. The study of Ref. 43 is the only one that contains information about the $(\gamma,x\gamma')$ experiment for the ^{30}Si nucleus. The data of this study are given in Tables XVI and XVII. The probability of occupation of excited states of the ^{29}Al nucleus as a result of the (γ,p) reaction is about 60%. Assuming that all the important partial transitions to excited ^{29}Al levels were identified in Ref. 43, we estimate $\sigma^{int}(\gamma,p_0)$ as the difference of $\sigma^{int}(\gamma,p)$ and $\Sigma_{i>1}\sigma^{int}(\gamma,p_i)$, and this gives

$$\sigma^{int}(\gamma,p_0)\simeq 45 \text{ MeV·mb up to } E_\gamma=26 \text{ MeV}.$$

This value, which is 40% of $\sigma^{int}(\gamma,p)$, is given in Table XVI.

The large value of $\sigma^{int}(\gamma,p_0)$ for ^{30}Si (as also for ^{29}Si) can be explained naturally by the very large value of the spectroscopic factor of the ground state of the final nucleus. For example, in the case of ^{29}Al, the fraction of the ground state corresponds to about 80% of the spectroscopic strength of the proton hole in the $1d_{5/2}$ shell of the ^{30}Si nucleus in the ground state. Thus, the ^{29}Al ground state is close to a pure hole state, and $\sigma^{int}(\gamma,p_0)$ must be formed by the semidirect decay of the GDR.

TABLE XIII. Integrated cross sections of the $^{28}Si(\gamma,n_i)^{27}Si$ reaction (Refs. 31 and 38–40), their semidirect components $\sigma^{int}_{s\,dir}$, and characteristics of the occupied states of the ^{27}Si nucleus (Ref. 26). $E^{m}_{\gamma}=28$ MeV.

Characteristics of ^{27}Si levels ($T=1/2$)					$\sigma^{int}(\gamma,n_i)$, MeV·mb		$\sigma^{int}_{s\,dir}(\gamma,n_i)$, MeV·mb
i	E_i, MeV	J^{π}	nlj	C^2S_i	(Ref. 31)	(Refs. 38–40)	
0	0	$5/2^+$	$1d_{5/2}$	3.45		42–52	42–52
1	0.78	$1/2^+$	$2s_{1/2}$	0.65	14±5	14–15	14–15
2	0.96	$3/2^+$	$1d_{3/2}$	0.60	7±2	7–8	7–8
3	2.16	$7/2^+$	—	—	—	—	
4	2.65	5.2^+	$1d_{5/2}$	0.50	<2.3	1.4–2.4	0.7–0.9
5	2.87	$3/2^+$	$1d_{3/2}$	0.55	3.4±1	2.3–3.2	1.5–1.7
6	2.91	$9/2^+$	—	—	—		
7	3.54	$1/2^+$	$2s_{1/2}$	0.01	—	0.2	
8	3.81	$3/2^+$	$1d_{3/2}$	—	—	0.8	
9	4.13	$1/2^-$	$1p_{1/2}$	1.6	—		≤0.8
10	4.29	$5/2^+$	$1d_{5/2}$	0.25	—	0.05	≤0.02
14	5.23	$3/2^-$	$1p_{3/2}$	1.8	—		—
		$\sigma^{int}(\gamma,n)$				70–80 (Refs. 38–40)	

TABLE XIV. Integrated cross sections of the $^{29}Si(\gamma,p_i)^{28}Al$ reaction (Ref. 43), their semidirect components $\sigma^{int}_{s\ dir}$, and characteristics of the occupied ^{28}Al levels (Ref. 26). E^m_γ=26 MeV.

Characteristics of the ^{28}Al levels(T=1)					$\sigma^{int}(\gamma,p_i)$, MeV·mb (Ref. 43)	$\sigma^{int}_{s\ dir}(\gamma,p_i)$, MeV·mb
i	E_i, MeV	J^π	nlj	C^2S_i		
0	0	3^+	$1d_{5/2}$	3.58	≈100*	≈100
1	0.03	2^+				
2	0.97	0^+	$2s_{1/2}$	0.04	10.0±3.5	0.12–0.16
3	1.01	3^+	$1d_{5/2}$	0.20	8.1±5.8	3.2–3.3
4	1.37	1^+	$2s_{1/2}$	0.47	25.0±4.5	1.25–1.6
5	1.620	1^+	$1d_{5/2}$	0.25	17.7±2.2	2.7–2.8
6	1.623	$2^+(3^+)$			14.7±2.3	
7	2.14	2^+	—	—	12.2±3.7	
8	2.20	1^+	$1d_{5/2}$	0.60	8.5±2.5	4.1–4.2
10	2.49	2^+	$1d_{5/2}$	0.27	12.3±1.7	1.45–1.49
12	2.66	$(2\text{-}4)^+$	$1d_{5/2}$	≤0.1	—	≤0.23
13	2.99	$(1.3)^+$	$1d_{5/2}$	0.36	—	1.2
14	3.01	0^+				
17	3.35	2^+	$1d_{5/2}$	0.19	2.5±1.7	0.43–0.45
19	3.54	1^+	$2s_{1/2}$	0.09	—	0.09–0.12
		$\sigma^{int}(\gamma,p)$			197–226 (Refs. 43 and 44)	

It is found that $\Sigma_i\sigma^{int}(\gamma,n_{i\geq 1}) \simeq 180$ MeV·mb (Ref. 43), and this value greatly exceeds the value $\sigma^{int}(\gamma,n+\gamma,np)$=137 MeV·mb obtained in the experiment that measured the total photoneutron cross section in a beam of quasimonochromatic photons.[45] We introduce the coefficient K by which it is necessary to multiply all the partial cross sections in order to bring their sum into agreement with the total photoneutron cross section. We determine the value of this coefficient from the revised value of $\sigma^{int}(\gamma,n_2)$. This last value was estimated from $\sigma^{int}(\gamma,p_0)$ under the assumption that (γ,p_0), like (γ,n_2), is entirely formed by semidirect processes. This gave $\sigma^{int}(\gamma,n_2)\simeq$19 MeV·mb. In this way, the value of K was found to be 19/35.3≃0.53.

The renormalized values of $\sigma^{int}(\gamma,n_i)$ are given in the second column on the right of Table XVII. The data of this column are used below to estimate $\sigma^{int}_{s\ dir}(\gamma,n_i)$. In its turn, the cross section $\sigma^{int}(\gamma,n_0)$ was estimated as the difference of $\sigma^{int}(\gamma,n)$ and $\Sigma_i\sigma^{int}(\gamma,n_{i\geq 1})$, where the renormalized values were taken for $\sigma^{int}(\gamma,n_i)$. The value $\sigma^{int}(\gamma,n_0)\simeq$35 MeV·mb was obtained. Under the assumption that the (γ,p_1) reaction is entirely formed by semidirect processes, the upper limit for $\sigma^{int}(\gamma,n_0)$ was found to be 64 MeV·mb, and this is a value that is consistent with the value 35 MeV·mb given above.

In the calculation of the semidirect components, we took $E(T_<)$=17.0 MeV, $E(T_>)$=21.0 MeV, $\sigma_<$=0.58, $\sigma_>$=0.42. The experimental data are reproduced best by the following set of parameters: a=0.97–1.0, $b_<\simeq$1, and $b_>$=0.7–0.9. The probabilities of the semidirect processes in the proton and neutron channels of the decay of the GDR of the ^{30}Si nucleus were found to be 0.57 and 0.71–0.73, respectively.

However, we cannot entirely rule out the possibility that $\sigma^{int}_{s\ dir}(\gamma,p_2)$ and $\sigma^{int}_{s\ dir}(\gamma,p_4)$ are appreciably greater than the values given in Table XVI. The occupied levels of ^{29}Al with i=2 and 4 contain an appreciable fraction of the spectroscopic strength of the $1d_{3/2}$ proton hole, and there is a correlation between C^2S_i and $\sigma^{int}(\gamma,p_i)$ for i=2 and 4. In addition, the levels with i=3 and 6, which lie in the same energy region but do not have a hole nature, are not occupied in the proton decay of the GDR of the ^{30}Si nucleus. All this indi-

TABLE XV. Integrated cross sections of the $^{29}Si(\gamma,n_i)^{28}Si$ reaction (Ref. 43), their semidirect components $\sigma^{int}_{s\ dir}$, and characteristics of the occupied ^{28}Si levels (Ref. 26). E^m_γ=26 MeV.

Characteristics of the ^{28}Si levels					$\sigma^{int}(\gamma,n_i)$, MeV·mb (Ref. 43)	$\sigma^{int}_{s\ dir}(\gamma,n_i)$, MeV·mb
i	E_i, MeV	$J^\pi T$	nlj	C^2_iS		
0	0	0^+0	$2s_{1/2}$	0.55	20–25*	20–25
1	1.78	2^+0	$1d_{5/2}$	0.51	47.0±6.0*	46.0–47.0
2	4.62	4^+0	—	—	1.9±1.8	—
3	4.98	0^+0	$2s_{1/2}$	0.08	9.2±1.8	1.9
4	6.28	3^+0	$1d_{5/2}$	0.45	23.9±4.0	13.4–13.6
11	7.93	2^+0	$1d_{5/2}$	0.13	1.7±1.3	0.7
20	9.32	3^+1	$1d_{5/2}$	0.7	15.1±2.5	5.0-5.2
21	9.38	2^+1	$1d_{5/2}$	0.33	15.6±2.0	2.2
		$\sigma^{int}(\gamma,n+\gamma,np)$			137±14 (Ref.45)	

TABLE XVI. Integrated cross sections of the $^{30}Si(\gamma,p_i)^{29}Al$ reaction (Ref. 43), their semidirect components $\sigma^{int}_{s\,dir}$, and characteristics of the occupied ^{29}Al levels (Refs. 26 and 46). $E^{m}_{\gamma}=26$ MeV.

Characteristics of the ^{29}Al levels ($T=3/2$)					$\sigma^{int}(\gamma,p_i)$, MeV·mb (Ref. 43)	$\sigma^{int}_{s\,dir}(\gamma,p_i)$, MeV·mb
i	E_i, MeV	J^{π}	nlj	C^2S_i		
0	0	$5/2^+$	$1d_{5/2}$	4.8	≅45*	45
1	1.40	$1/2^+$	$2s_{1/2}$	0.7	25.4±2.2	14
2	1.75	$(3/2,7/2)^+$	$(1d_{3/2})$	0.2	7.2±2.5	0.09–0.15(7.2)
4	2.87	$3/2^+$	$1d_{3/2}$	0.6	12.0±3.2	0.1–0.2(10.7)
5	3.06	$5/2^+$	$1d_{5/2}$	1.05	5.8±2.5	3.0
7	3.43	$1/2^+$	$2s_{1/2}$	0.13	—	0.09
9 10	3.64 3.67	$(3/2,5/2)^+$	$(1d_{3/2,5/2})$	0.25	—	0.01–0.5
14	4.22	$5/2^+$	$1d_{5/2}$	0.24	1.1±1.0	0.3
15	4.40	$(3/2-9/2)^+$	—	—	11.8±5.0	
		$\sigma^{int}(\gamma,p)$			93–127 (Refs. 43 and 44)	

cates a semidirect nature of the (γ,p_2) and (γ,p_4) channels and forces us to consider one further way of calculating $\sigma^{int}_{s\,dir}(\gamma,p_2)$ and $\sigma^{int}_{s\,dir}(\gamma,p_4)$ in which $\sigma^{int}(\gamma,p_2)$ is taken as the base cross section. The new estimates of $\sigma^{int}_{s\,dir}(\gamma,p_2)$ and $\sigma^{int}_{s\,dir}(\gamma,p_4)$ are given in the brackets in the extreme right-hand column of Table XVI. These values are to be regarded as the upper limits of $\sigma^{int}_{s\,dir}(\gamma,p_i)$ for $i=2$ and 4. At the same time, for the upper limit on the probability of the semidirect processes in the proton channel of the decay of the GDR of the ^{30}Si nucleus, we obtain the value 0.77.

It should, however, be emphasized that the choice of $\sigma^{int}(\gamma,p_2)$ instead of $\sigma^{int}(\gamma,n_1)$ as the base cross section in the calculation of the semidirect components of the cross sections for occupation of levels containing an admixture of a hole in the $1d_{3/2}$ shell gives for $\sigma^{int}_{s\,dir}(\gamma,n_1)$ and $\sigma^{int}_{s\,dir}(\gamma,n_3)$ values that greatly exceed the experimental values. With allowance for everything said above, we must expect for the probability of semidirect processes in the photoproton channel of the decay of the GDR of the ^{30}Si nucleus a value at the level 0.57 (certainly ≤0.77).

All the observed partial transitions correspond to excitation of nucleons of the $1d2s$ shell, i.e., they correspond to transitions of group A. Up to 26 MeV, the contribution of transitions of group B is small.

3.6. The ^{31}P nucleus

Many studies have been made of the partial channels of the decay of the GDR of this nucleus. Three $(\gamma,x\gamma')$ experiments were made.[12,47,48] From the spectra of photonucleons measured with different upper limits of the bremsstrahlung spectrum, energy dependences were obtained for the cross sections of the (γ,p_i) reaction[49,50] and the (γ,n_i) reaction.[51] In Ref. 52, the cross section of the $^{30}Si(p,\gamma_0)^{31}P$ reaction was measured using a beam of polarized protons. Our analysis was based mainly on the data of the most complete experiments[47,50] using some data from Refs. 12, 48, and 51 (see Tables XVIII and XIX).

Comparison of the data for the $(\gamma,p\gamma')$ (Ref. 47) and (γ,p_i) (Ref. 50) experiments (Table XVIII) reveals a large difference in the values of $\sigma^{int}(\gamma,p_i)$ for $i=1$ and 2 and to a lesser degree for the group of states with $i=5$–11. However, the data of Ref. 47 are consistent with the analogous data obtained by the $(\gamma,x\gamma')$ method,[12,48] and the data of Ref. 50

TABLE XVII. Integrated cross sections of the $^{30}Si(\gamma,n_i)^{29}Si$ reaction (Ref. 4), their semidirect components $\sigma^{int}_{s\,dir}$, and characteristics of the occupied ^{29}Si levels (Refs. 26 and 46). $E^{m}_{\gamma}=26$ MeV.

Characteristics of the ^{29}Si levels					$\sigma^{int}(\gamma,n_i)$, MeV·mb		$\sigma^{int}_{s\,dir}(\gamma,n_i)$, MeV·mb
i	E_i, MeV	$J^{\pi}T$	nlj	C^2S_i	(Ref. 43)	$K=0.53$	
0	0	$1/2^+\,1/2$	$2s_{1/2}$	0.89		≅35*	35
1	1.27	$3/2^+\,1/2$	$1d_{3/2}$	0.87	60.1±4.0	32*	32
2	2.03	$5/2^+\,1/2$	$1d_{5/2}$	1.5	35.3±3.8	19	19
3	2.43	$3/2^+\,1/2$	$1d_{3/2}$	0.19	28.1±2.0	15	3.4–5.7
4	3.07	$5/2^+\,1/2$	$1d_{5/2}$	0.15	17.1±4.0	9.1	0.9
5	3.62	$7/2^-\,1/2$	$1f_{7/2}$	0.10	10.5±1.8	5.6	
8	4.84	$1/2^+\,1/2$	$2s_{1/2}$	0.14	8.6±2.4	4.6	1.7
9	4.90	$5/2^+\,1/2$	$1d_{5/2}$	0.84	7.9±2.7	4.2	0.4
10	4.93	$3/2^-\,1/2$	—	—	4.5±2.0	2.4	
16	6.11	$(3/2,5/2)^+\,1/2$	—	—	6.2±2.4	3.3	
47	8.33	$5/2^+\,3/2$	$1d_{5/2}$	2.35	<0.5	<0.3	≅0
		$\sigma^{int}(\gamma,n)$			130±15 (Refs. 43 and 45)		

The column headed $K=0.53$ gives the data of Ref. 43 multiplied by the coefficient 0.53.

TABLE XVIII. Integrated cross sections of the $^{31}P(\gamma,p_i)^{30}Si$ reaction (Refs. 47 and 50), their semidirect components $\sigma^{int}_{s\,dir}$, and characteristics of the occupied ^{30}Si levels (Ref. 26).

Characteristics of the ^{30}Si levels ($T=1$)					$\sigma^{int}(\gamma,p_i)$, MeV·mb		
i	E_i, MeV	J^π	nlj	C^2S_i	$(\gamma,p\gamma')$ (Ref. 47) $E^m_\gamma=32$ MeV	(γ,p) (Ref. 50) $E^m_\gamma=25$ MeV	$\sigma^{int}_{s\,dir}(\gamma,p_i)$, MeV·mb
0	0	0^+	$2s_{1/2}$	0.5		16*	16
1	2.24	2^+	$1d_{5/2}$	1.7	100±13	11.3*	12
2	3.50	2^+	$1d_{5/2}$	0.5	59±11		2.8
3	3.77	1^+	—	—	12.6±2.5	9.7	
4	3.79	0^+	$2s_{1/2}$	0.04	—		0.9
5	4.81	2^+	$1d_{3/2}$	0.007	18.8±5.7		
6	4.83	3^+	$1d_{5/2}$	0.17	11.1±2.5		0.6
7	5.23	3^+	$1d_{5/2}$	1.2	7.0±2.5		3.4
8	5.28	4^+	—	—	6.0±2.0	28.8	
9	5.37	0^+	$2s_{1/2}$	0.14	3.0±1.0		2.3
10	5.49	3^-	—	—	18.6±4.4		
11	5.61	2^+	$1d_{5/2}$	0.31	15.3±4.4		0.75
14	6.54	2^+	$1d_{5/2}$	0.25	5.8±1.8		0.4
16	6.74	1^-	—	—	—	18.3	
18	6.87	3^+	$1d_{5/2}$	0.59	11.3±1.5		0.75
22	7.08	$3^+(1^+)$	$1d_{5/2}$	0.22	—		0.25
23	7.26	2^+	$1d_{5/2}$	0.12	11.3±3.8		0.13
27	7.63	2^+	—	—	4.9±1.9		
28	7.67	$(1-3)^+$	$1d_{5/2}$	0.37	2.3±0.6		0.25
	8.14		$1d_{5/2}$	0.27	—		
	8.78		$1d_{5/2}$	0.14	—	24	
43	8.90	1^-	—	—	13.8±7.5		
	8.92		$1d_{5/2}$	0.15	—		
44	8.95		$1d_{5/2}$	—	—		
50	9.25	$(1-3)^+$	$1d_{5/2}$	0.18	—		
	≥9.5		—	—	—	90–150	
$\sigma^{int}(\gamma,p+\gamma,np)$					330±50 (Ref. 55, $E^m_\gamma=30$ MeV)		

agree with the data of other $(\gamma,p_{i=0,1})$ experiments.[49,52] This contradiction was analyzed in Refs. 53 and 54. The conclusion was that the data of the (γ,p_i) experiments should be regarded as correct. The large values of $\sigma^{int}(\gamma,p_i)$ for the low-lying excited states (especially for $i=1$ and 2) obtained in the $(\gamma,p\gamma')$ experiments[12,47,48] can be explained by the fact that in them it was not possible to take into account fully the contribution of the γ transitions from high-lying (≥9.5 MeV) states of ^{30}Si with $J^\pi=1^-$ to low-lying ^{30}Si levels. Such γ transitions have energy 7–10 MeV and are in a region in which the γ-ray detection efficiency of the Ge(Li) detector is low. At the same time, in the $^{31}P(\gamma,p)^{30}Si$ reaction the final nucleus in about 50% of the cases is in fact in a state with excitation energy above 9.5 MeV. The data of the $(\gamma,p\gamma')$ and (γ,p_i) experiments for $i>11$ are mutually consistent.

It follows from Table XVIII that $\Sigma_i\sigma^{int}(\gamma,p_i) \simeq 320$ MeV·mb, where for $i>0$ the values of $\sigma^{int}(\gamma,p_i)$ obtained in the $(\gamma,p\gamma')$ experiment of Ref. 47 have been used. This value agrees well with the value

$$\int_0^{30}\sigma(\gamma,p+\gamma,np)dE_\gamma=330\pm50 \text{ MeV·mb}$$

obtained in Ref. 55 and indicates that the experiment of Ref. 47 identified practically all the proton decays from the GDR of the ^{31}P nucleus to excited levels of the ^{30}Si nucleus with $i=1$ and 2, and an appreciable fraction of the decays to the levels with $i=5-11$ is indeed due to the predominant occupation in the decay of the GDR of ^{30}Si levels having excitation energy above 9.5 MeV.

The integrated total photoneutron cross section was determined in several experiments (in particular, in Ref. 19). Averaging of the results of these experiments gives

$$\int_0^{30}\sigma(\gamma,n+\gamma,np+\gamma,2n)dE_\gamma\simeq200\pm30 \text{ MeV·mb},$$

and, in accordance with Ref. 19, $\int_0^{30}\sigma(\gamma,np)dE_\gamma\simeq55$ MeV·mb, while $\int_0^{30}\sigma(\gamma,2n)dE_\gamma$ is small and can be ignored.

We also give some explanations of the experimental data given in Table XVIII. The value $\sigma^{int}(\gamma,p_0)=16$ MeV·mb exceeds by 20% the value given in Ref. 50, since it takes into account the contribution of $\sigma(\gamma,p_0)$ in the region from the threshold to 14.6 MeV [in this region, $\sigma(\gamma,p_0)$ was not determined in Ref. 50]. In Ref. 50, there was also no determination of $\sigma^{int}(\gamma,p_0)$ for $E_i\geq9.5$ MeV. The value 90–150 MeV·mb given for this cross section in Table XVIII was obtained by subtracting $\Sigma_i\sigma^{int}(\gamma,p_{i\leq50}) = 108$ MeV·mb (data in the second column on the right in the table) from $\sigma^{int}(\gamma,p)$ up to 25 MeV estimated in accordance with the data of Refs. 50 and 55 after subtraction of $\int_0^{25}\sigma(\gamma,np)dE_\gamma\simeq25$

TABLE XIX. Integrated cross sections of the $^{31}P(\gamma,n_i)^{30}P$ reaction (Refs. 12, 47, 48, and 51), their semidirect components $\sigma^{int}_{s\ dir}$, and characteristics of the occupied ^{30}P levels (Ref. 26).

Characteristics of the ^{30}P levels					$\sigma^{int}(\gamma,n_i)$, MeV·mb			
i	E_i, MeV	$J^\pi T$	nlj	C^2S_i	$(\gamma,n\gamma')$ (Ref. 47) E^m_γ=32 MeV	$(\gamma,n\gamma')$ (Refs. 12 and 48) E^m_γ=30 MeV	(γ,n) (Ref. 51) E^m_γ=23 MeV	$\sigma^{int}_{s\ dir}(\gamma,n_i)$, MeV·mb
0	0	1^+0	$2s_{1/2}$	0.66			≅40	63.2
			$1d_{3/2}$	0.13				8.7
1	0.68	0^+1	$2s_{1/2}$	0.25		25±4 (Ref. 48)		23.2
2	0.71	1^+0	$2s_{1/2}$	0.11		30±8 (Ref. 48)		9.6
			$1d_{3/2}$	0.46		39±10 (Ref. 12)		27.1
3	1.45	2^+0	$1d_{3/2}$	0.47	24.1±11.3*			23.9
4	1.97	3^+0	$1d_{5/2}$	0.75	44.8±8.8			13.3
5	2.54	3^+0	$1d_{5/2}$	0.65	11.7±4.0			10.0
6	2.72	2^+0	$1d_{5/2}$	0.49	2.3–7.7			7.2
8	2.94	2^+1	$1d_{5/2}$	0.67	8.3±3.3			8.8
9	3.02	1^+0	$2s_{1/2}$	0.07	6.8±1.8			3.9
			$1d_{3/2}$	0.12				4.0
12	3.83	2^+0	$2s_{1/2}$	0.03	11.3±3.8			10.3
			$1d_{3/2}$	0.41				
15	4.18	2^+1	$1d_{5/2}$	0.25	8.0±2.6			1.9
20	4.42	2^+0	$1d_{5/2}$	0.44	3.0±1.3			3.1
21	4.47	0^+1	$2s_{1/2}$	0.02				1.2
22	4.50	1^+1	$1d_{3/2}$	0.003	3.5±1.3			
24	4.74	$(1.3)^+0$	$1d_{5/2}$	0.06	8.3±1.5			
28	5.21	$(1-3)^+0$	$1d_{5/2}$	0.24				0.9
31	5.51	$(2.3)^+1$	$1d_{5/2}$	0.11	3.4±1.3			0.25
32	5.59	2^+1	$1d_{3/2}$					
33	5.71	1^+0	$2s_{1/2}$	0.05				
35	5.89	$(1-3)^+1$	$1d_{5/2}$	0.67				1.1
38	6.00	1^+0	$1d_{5/2}$	1.6				0
39	6.05	0^+1	$2s_{1/2}$	0.1				0
		$\sigma^{int}(\gamma,n+\gamma,np)$ / $\sigma^{int}(\gamma,n)$					200±30 (Ref. 19) / 140–150 (Ref. 19) E^m_γ=30 MeV	

MeV·mb (Ref. 19). The interval 90–150 MeV·mb takes into account the difference between the data of Refs. 50 and 55.

The summed partial photoneutron cross sections give

$$\sum_{i=0}^{31} \sigma^{int}(\gamma,n_i)=230-245 \text{ MeV·mb}.$$

This value exceeds the value given above (200±30 MeV·mb) for the integrated cross section of the total photoneutron reaction. This indicates that in the neutron decay of the GDR of the ^{31}P nucleus there is practically no occupation of levels of the final ^{30}P nucleus with $i>32$.

Details of the calculation of the semidirect components are described in Ref. 54. Its results, with small corrections, are given in Tables XVIII and XIX. They correspond to values $a=1$, $b_>=1$, $b_<=0.6$ for the levels with hole configurations $1d^{-1}_{5/2}$ and $1d^{-1}_{3/2}$. For $E(T_<)$ and $E(T_>)$, the values 18.3 and 21.2 MeV were taken, and $\sigma_<$ and $\sigma_>$ were taken equal to 0.38 and 0.62, respectively. Good agreement of $\sigma^{int}_{s\ dir}(\gamma,n_i)$ for $i=0$, 1, and 2 with the available experimental data[12,48,51] was obtained (see Table XIX). This indicates that the semidirect components are dominant in these neutron channels.

The contribution of the semidirect processes in the photoproton reaction was found to be 0.16–0.21 (E^m_γ=25 MeV), and in the photoneutron reaction it was 0.80–0.85 (E^m_γ=30–32 MeV).

According to the data of the single-nucleon transfer reaction, levels containing a significant fraction of the spectroscopic strength of hole excitations in the $1p$ shell are not observed in the final nuclei. This means that all the partial transitions represented in these tables are due to dipole transitions from outer shells of the ^{31}P nucleus. Such transitions exhaust the entire neutron cross section and are not less than 42% of the proton cross section (up to E_γ=25 MeV).

3.7. The ^{32}S nucleus

The most complete information about the partial nucleon channels of the decay of the GDR in ^{32}S was obtained in the (γ,p_i) experiment of Ref. 56 and in two $(\gamma,x\gamma')$ experiments.[57–59] In Ref. 59, the data of the experiments of Refs. 56, 58, and 59 were used to determine the energy dependences of the (γ,n_i) cross section. Data of these studies are given in Tables XX and XXI.

In the experiments of Refs. 56–59, the GDR decay prod-

TABLE XX. Integrated cross sections of the $^{32}S(\gamma,p_i)^{31}P$ reaction (Refs. 56–59), their semidirect components $\sigma^{int}_{s\,dir}$, and characteristics of the occupied ^{31}P levels (Ref. 26).

Characteristics of the ^{31}P levels ($T=1/2$)					$\sigma^{int}(\gamma,p_i)$, MeV·mb			
i	E_i, MeV	J^π	nlj	C^2S_i	(γ,p) (Ref. 56) $E^m_\gamma=29$ MeV	$(\gamma,p\gamma')$ (Ref. 57) $E^m_\gamma=26$ MeV	$(\gamma,p\gamma')$ (Refs. 58 and 59) $E^m_\gamma=32$ MeV	$\sigma^{int}_{s\,dir}(\gamma,p_i)$, MeV·mb
0	0	$1/2^+$	$2s_{1/2}$	1.0	16*			16
1	1.27	$3/2^+$	$1d_{3/2}$	0.75	48	48±12	47±9*	47
2	2.23	$5/2^+$	$1d_{5/2}$	2.1	29	25±4	28±6*	28
3	3.13	$1/2^+$	$2s_{1/2}$	0.13		11±1	11±1	0.9
4	3.30	$5/2^+$	$1d_{5/2}$	0.6	39	13±1	15±1	5.4–6.9
5	3.41	$7/2^+$	—	—		3.3±0.6	3.1±0.6	
6	3.51	$3/2^+$	$1d_{3/2}$	—		10±3	13±3	
7	4.19	$5/2^+$	$1d_{5/2}$	0.6		6±1	9±1	3.5–5.5
8	4.26	$3/2^+$	$1d_{3/2}$	—		13±5	10±3	
9	4.43	$7/2-$	$1f_{7/2}$	(0.04)				
10	4.59	$3/2^+$	$1d_{3/2}$	0.2	44	5±1	7.5±2.5	
11	4.78	$5/2^+$	$1d_{5/2}$					0.9–1.6
13–14	5.01	3/2		0.1		(9±4)	6±1	
16	5.26	$1/2^+$	$2s_{1/2}$			5±1	4.4±2.5	0.4
19	5.56	$3/2^+$	$1d_{3/2}$	0.15		3.8±1.9	5.0±2.5	
	5.91		$(1d_{5/2})$	0.14				0.4–0.9
23	5.99	$3/2^-$	$(1d_{5/2})$			(3.8±2.5)	5±1	0.3–0.9
27	6.34	$1/2^+$	$2s_{1/2}$	0.11			6.3±2.5	0.2
40	6.91	$\left(\frac{1}{2},\frac{3}{2}\right)^-$		0.79	51		(5.0±2.5)	
46	7.21	$\left(\frac{1}{2},\frac{3}{2}\right)^-$	$(1d_{5/2})$					1-3
	7.98		$(1p_{1/2})$	0.82				
	9.68		$(1d_{5/2})$	0.18	69			0.06–0.26
				0.15				
	9.97		$(1d_{5/2})$					0.04–0.2
	12.5				47			
		$\sigma^{int}(\gamma,p+\gamma,np)$ / $\sigma^{int}(\gamma,p)$					340–345 (Ref. 56) / ≅330 (Refs. 19 and 56)	($E^m_\gamma=29$ MeV)

ucts were detected at a definite angle to the direction of the primary γ beam (90° in the detection of the photoprotons in Ref. 56, and 140° and 150° in the detection of the secondary γ rays in Refs. 57–59). The values of $\sigma^{int}(\gamma,x_i)$ given in Tables XX and XXI for Refs. 57–59 were obtained by multiplying the differential cross sections by 4π. For Ref. 56, the values of $\sigma^{int}(\gamma,p_i)$ given in Table XIX were obtained by integrating over the angle with allowance for the experimental angular distribution.

The total integrated cross sections for the photoproton and photoneutron transitions observed in the $(\gamma,x\gamma')$ experiment [with allowance for the (γ,p_0) and (γ,n_0) channels] are 191±14 and 57±11 MeV·mb. At the same time, the integrated cross sections of the (γ,p) and (γ,n) reactions up to 29 MeV are ≈330 and 95 MeV·mb, respectively. Thus, an appreciable fraction of the photonucleon transitions in the $(\gamma,x\gamma')$ experiment was not separated. This applies mainly to transitions to highly excited levels with $E_i\geq 6$ MeV of the ^{31}P nucleus and with $E_i\geq 4$ MeV of the ^{31}S nucleus. The deficit of photonucleon decays in the $(\gamma,x\gamma')$ experiment to ^{32}S cannot be ascribed to the (γ,np) and $(\gamma,2n)$ two-nucleon reactions. According to the data of Ref. 19, in the region $E_\gamma\leq 29$ MeV we have $\sigma^{int}(\gamma,np)\simeq 11$ MeV·mb, while $\sigma^{int}(\gamma,2n)\simeq 0$ ($B_{2n}=28.1$ MeV).

The procedure for calculating $\sigma(\gamma,n_i)$ from the experimental values of $\sigma(\gamma,p_i)$ (Ref. 59) made it possible to establish the orbital angular momentum of the photonucleons. This showed that in the region $E_\gamma<20.5$ MeV there is predominant emission of photonucleons with $l=1$, i.e., shell configurations of the type $(1d2s)^{-1}2p$ are predominant in the GDR. At $E_\gamma>20.5$ MeV, photonucleons with various l (from 0 to 3) are emitted.

In the calculation, the cross sections of the (γ,p_0), (γ,p_1), and (γ,p_2) reactions were taken as the base cross sections. A fluctuation analysis of the fine structure of the cross section of the (p,γ_0) reaction on the ^{31}P nucleus made in Ref. 60 showed that the probability of semidirect decay in the ^{32}S (γ,p_0) channel is about 90%.

It follows from Tables XX and XXI that $\Sigma_i\sigma^{int}_{s\,dir}(\gamma,p_i)=104-112$ MeV·mb, while $\Sigma_i\sigma^{int}_{s\,dir}(\gamma,n_i)=55-79$ MeV·mb. At the same time, we assumed that the proton transitions to the states of the ^{31}P nucleus with $E_i>10$ MeV are not formed by the semidirect mechanism of decay

TABLE XXI. Integrated cross sections of the $^{32}S(\gamma,n_i)^{31}S$ reaction (Refs. 57–59), their semidirect components $\sigma^{int}_{s\ dir}$, and characteristics of the occupied states of the ^{31}S final nucleus.[26]

	Characteristics of the ^{31}S levels ($T=1/2$)				$\sigma^{int}(\gamma,n_i)$, MeV·mb			
					Converted from (γ,p_i)	(γ,p_i)		
i	E_i, MeV	J^π	nlj	C^2S_i	$E^m_\gamma=29$ MeV (Ref. 59)	$E^m_\gamma=26$ MeV (Ref. 57)	$E^m_\gamma=32$ MeV (Refs. 58 and 59)	$\sigma^{int}_{s\ dir}(\gamma,n_i)$, MeV·mb
0	0	$1/2^+$	$2s_{1/2}$	0.95	≅10			≅10
1	1.25	$3/2^+$	$1d_{3/2}$	0.8	17–36	24±3	21±7	21-24
2	2.24	$5/2^+$	$1d_{5/2}$	2.2	8-20	13±4	24±6	13-24
3	3.08	$1/2^+$	$2s_{1/2}$	0.14	6			0.5
4	3.29	$5/2^+(3/2^+)$	$1d_{5/2}$	0.7	3.1–7.4			1.5–4.5
5	3.35	$(3/2,7/2)^+$			0.2–0.8	1.9±1.3	2.1±0.6	
6	3.44	$3/2^+$	$1d_{3/2}$		2.6–6.0			
7	4.08	$(3/2,5/2)^+$	$1d_{5/2}$	0.85	1.5–4.0			1.3–4.1
8	4.21				1.5–4.5			
10	4.53	$(3/2,5/2)^+$	$1d_{3/2}$		1.1–3.0			
12	4.72	$(3/2,5/2)^+$	$1d_{5/2}$	0.45	0.3–1.1			0.5–1.8
14	4.97	$(1/2,3/2)^-$		0.06	1.4–2.8			2.8
16	5.15	$1/2^+$	$2s_{1/2}$	0.32	1.6			0.4
22	5.78	$(3/2,5/2)^+$	$1d_{5/2}$	0.27				0.2–0.7
24	5.89	$(3/2,5/2)^+$	$1d_{5/2}$	0.20				0.1–0.5
27	6.27	$1/2^+$	$2s_{1/2}$	0.22	3–16			0.1
40	6.99	$1/2^+$	$2s_{1/2}$	0.05				0.02
41	7.04	$(3/2,5/2)^+$	$1d_{5/2}$	1.0				0.3–1.6
43	7.17	$(3/2,5/2)^+$	$1d_{5/2}$	0.21				0.06–0.8
	9.68		$(1d_{5/2})$	0.18	1.4–11			0.01–0.0
	9.97		$(1d_{5/2})$	0.15				<0.06
	12.5				3.1			<3.1
		$\sigma^{int}(\gamma,n)$				95±10 (Ref. 19) ($E^m_\gamma=29$ MeV)		

of the GDR, since in this energy region there are only hole excitations in the $1p$ shell of the ^{32}S nucleus. These are strongly spread over the levels of the final nucleus, so that their weight in the wave functions of these levels is small. A small fraction of semidirect decays of the $1p\rightarrow 1d2s$ branch of the GDR of the ^{32}S nucleus is also indicated by the theoretical calculations of Ref. 61. The probability of semidirect processes in the (γ,p) and (γ,n) reactions for the ^{32}S nucleus is estimated at 0.31–0.35 and 0.58–0.83, respectively. The probability of semidirect processes in the total cross sections

TABLE XXII. Integrated cross sections of the $^{39}K(\gamma,p_i)^{38}Ar$ reaction (Ref. 62), their semidirect components $\sigma^{int}_{s\ dir}$, and characteristics of the occupied states of the ^{38}Ar final nucleus (Refs. 26 and 46). $E^m_\gamma=32$ MeV.

	Characteristics of the ^{38}Ar levels ($T=1$)				$\sigma^{int}(\gamma,p_i)$, MeV·mb	$\sigma^{int}_{s\ dir}(\gamma,p_i)$, MeV·mb
i	E_i, MeV	J^π	nlj	C^2S_i		
0	0	0^+	$1d_{3/2}$	0.67		29.5
1	2.17	2^+	$2s_{1/2}$	0.05	72.5±4*	
			$1d_{3/2}$	2.8		72.5
2	3.88	0^+	$1d_{3/2}$	0.01	8.2±3	0.18
3	3.81	3^-	$1f_{7/2}$	0.01	20.9±4	≅0
4	3.94	2^+	$2s_{1/2}$	0.21	14.3±2.5	5
			$1d_{3/2}$	0.15		2.5
6	4.57	2^+	$2s_{1/2}$	0.56	36.1±9	11.9
			$1d_{3/2}$	0.30		3.8
9	4.88	3^-	$1f_{7/2}$	<0.03	10.1±1.3	≅0
11	5.16	2^+	$2s_{1/2}$	0.28	19.8±5	5
			$1d_{3/2}$	(0.2)		1.9
12	5.35	4^+	—	—	11.4±4.5	≅0
13	5.51	3	—	—	6.3±2.5	0
14	5.55	$(1,2)^+$	$2s_{1/2}$	0.7	29.9±6	11.8
		$\sigma^{int}(\gamma,p)$			260±20 (Ref. 62)	

TABLE XXIII. Integrated cross sections of the $^{39}K(\gamma,n_i)^{38}K$ reaction (Ref. 62), their semidirect components $\sigma^{int}_{s\,dir}$, and characteristics of the occupied states of the ^{38}K final nucleus (Refs. 26 and 46). $E^{m}_{\gamma}=32$ MeV.

Characteristics of the ^{38}K levels						
i	E_i, MeV	$J^{\pi}T$	nlj	C^2S_i	$\sigma^{int}(\gamma,n_i)$, MeV·mb	$\sigma^{int}_{s\,dir}(\gamma,n_i)$, MeV·mb
0	0	3^+0	$1d_{3/2}$	1.8	—	70.3
1	0.13	0^+1	$1d_{3/2}$	0.33	—	32.7
2	0.46	1^+0	$2s_{1/2}$	0.19	—	13.2
			$1d_{3/2}$	0.32		10.7
3	1.70	1^+0	$2s_{1/2}$	0.04	9.4±1.3	8.8
			$1d_{3/2}$	0.66		
			$2s_{1/2}$	0.03	42.7±6	
			$1d_{3/2}$	1.39		
4	2.40	2^+1	$2p_{3/2}$	0.03		47.7
			$1f_{7/2}$	0.08	9.2±2.5	0
6	2.65	$(2.4)^-0$	$2s_{1/2}$	0.56		
			$1d_{3/2}$	0.19	15.6±5*	15.6
						0.2
13	3.43	2^+0			160±20 (Ref. 19)	
		$\sigma^{int}(\gamma,n)$				

of the (γ,p) and (γ,n) reactions is 0.37–0.45. The calculation of Ref. 61 gives 0.40 for the probability of semidirect processes in the cross section for photoabsorption of the ^{32}S nucleus.

It follows from Tables XX and XXI that not less than 55% of the proton transitions and 93% of the neutron transitions are due to the $(1d2s)\rightarrow(1f2p)$ branch of the GDR of the ^{32}S nucleus.

3.8. The ^{39}K nucleus

The partial channels of photodisintegration of the ^{39}K nucleus have been investigated in a single $(\gamma,x\gamma')$ experiment.[62] The results of it are given in Tables XXII and XXIII. The experiment was made at detection angle 140° of the photons relative to the direction of the bremsstrahlung. The values of $\sigma^{int}(\gamma,x_i)$ given in the tables were obtained by multiplying by 4π the differential partial cross sections given in Ref. 62.

Details of the calculation for ^{39}K can be found in Ref. 62. The calculation was made for $E(T_<)=18.0$ MeV, $E(T_>)=20.3$ MeV, $\sigma_<=0.35$, $\sigma_>=0.65$. For the calculation of the semidirect components of the cross sections formed as a result of the presence in the occupied states of an admixture of a hole in the $1d_{3/2}$ subshell the cross section $\sigma^{int}(\gamma,p_1)$ was used, and for the case of an admixture of a hole in the $2s_{1/2}$ subshell the cross section $\sigma^{int}(\gamma,n_{13})$ was used. For levels having comparable C^2S_i for the $1d_{3/2}$ and $2s_{1/2}$ subshells, estimates corresponding to semidirect decay due to the presence of each of these hole components separately were obtained. The two estimates are given in the table. In the remaining cases, the calculation was made for the dominant hole component. The best description of the experimental data was obtained for $a=0.7$–0.8 and $b_<=b_>=1$. This means that in the semidirect decay of the GDR of the ^{39}K nucleus the ^{38}Ar and ^{38}K levels containing an admixture of a hole in the $1d_{3/2}$ subshell are occupied by the predominant emission of nucleons with $l=3$. Assuming that the (γ,p_0) and (γ,n_{1-3}) partial channels are formed by semidirect processes, we obtain from Tables XXII and XXIII the following estimates of the integrated cross sections of the (γ,p) and (γ,n) reactions up to $E_\gamma\simeq30$ MeV:

$$\sigma^{int}(\gamma,p)=\sum_i \sigma^{int}(\gamma,p_i)\simeq260\pm20 \text{ MeV·mb},$$

$$\sigma^{int}(\gamma,n)=\sum_i \sigma^{int}(\gamma,n_i)\simeq200\pm25 \text{ MeV·mb}.$$

According to the data of Ref. 19, in the same energy region ($E_\gamma\leqslant30$ MeV) the cross section is $\sigma^{int}(\gamma,n)\simeq160\pm20$ MeV·mb, in good agreement with the results of the $(\gamma,n\gamma')$ experiment. The integrated photoabsorption cross section according to the data of the $(\gamma,x\gamma')$ experiment is 480 MeV·mb [with allowance for the (γ,a) reaction[62]], and this is 80% of the classical dipole sum rule ($60NZ/A$ MeV·mb). All this indicates that the role of nucleon decays to states with higher excitation energy than those given in Tables XXII and XXIII is small. In particular, the role of nucleon decays to hole levels of the $1d_{5/2}$ subshell and the $1p$ shell is small.

It follows from Tables XXII and XXIII that the integrated probabilities of the semidirect processes for the (γ,p) and (γ,n) reactions are, respectively, 0.56 and 0.95. In the total cross section of the photonucleon reactions, this probability is 0.75.

3.9. The ^{40}Ca nucleus

The most complete information about the partial nucleon channels of decay of the GDR of the ^{40}Ca nucleus is contained in Refs. 63 and 64. Both studies use the $(\gamma,x\gamma')$ method. In addition, the energy dependences of the (γ,p_i) cross sections were determined in Ref. 63 from the spectra of photoprotons measured at different upper limits of the

TABLE XXIV. Integrated cross sections of the $^{40}Ca(\gamma,p_i)^{39}K$ and $^{40}Ca(\gamma,n_i)^{39}Ca$ reactions (Refs. 63 and 64), and characteristics of the occupied states of the final nucleus (Refs. 26 and 46).

	Characteristics of the ^{39}K and ^{39}Ca levels					$\sigma^{int}(\gamma,p_i)$ and $\sigma^{int}(\gamma,n_i)$, MeV·mb		
i	Nucleus	E_i, MeV	J^π	nlj	C^2S_i	$(\gamma,x\gamma')$ Ref. 64 E_γ^m=32 MeV	$(\gamma,x\gamma')$ Ref. 63 E_γ^m=30.25 MeV	(γ,x_i) Ref. 63 E_γ^m=24.6 MeV
0	K, Ca	0	$3/2^+$	$1d_{3/2}$	3.97	110–120	estimates	100±7
					5.4	40–50		38±4
1	K, Ca	2.52, 2.47	$1/2^+$	$2s_{1/2}$	1.65	61±2.1	59±4	49±5
					2.1	18.2±1.3	18±2	
2	K, Ca	2.81, 2.80	$7/2^-$	$1f_{7/2}$	0.53	18.5±3.4	17±2	only (γ,p) ↓
					0.44		3±2	
3	K, Ca	3.02, 3.03	$3/2^-$	$2p_{3/2}$	0.05	16.5±1.8	15±2	
					0.03			
4	K	3.60	$9/2^-$			3.6±1.7	2.3±1	
5	K	3.88	$3/2^-$	$2p_{3/2}$	0.02	3.4±1.4	2.9±0.7	50±5
6	Ca	3.87	$(3/2^+)$					
6	K	3.94	$3/2^+$			11±1.3	10.2±0.7	
8	Ca	3.94	$(3/2^-)$	$(2p_{3/2})$	0.04			
10	Ca	4.02	$1/2^+$	$2s_{1/2}$	0.09	4.2±2.4		
8	K	4.08	$3/2^-$	$(2p_{3/2})$		3.8±2.5	3.5±0.7	
13	Ca	4.49	$(5/2^+)$	$(1d_{5/2})$	0.1	1.7±0.9		
15	K	4.74	$(3/2^- - 7/2^{k+})$			3.8±1.8		
16	K	4.93	$3/2^+$			6.3±1.8	5.4±0.8	
22	K	5.26			1.0	6.4±1.5	6.5±1	
18	Ca	5.13	$5/2^+$	$1d_{5/2}$	1.3	0.9±0.9	2.0±0.7	
21	K	5.17	$(1/2-7/2^+)$			1.3±0.8		
23	K	5.32	$3/2^+$			4.0±1.1	3.8±1.6	
26	K	5.60			0.66	8.2±1.8	8±1	67±8
19	Ca	5.49	$5/2^+$	$1d_{5a/2}$	0.52	2.4±0.8	2.2±0.8	
28	K	5.71	$3/2^+$			1.8±0.9		
32	K	5.83	$(1/2,3/2^-)$	$(2p_{3/2})$	0.05	2.6±1.5	2±1	
34	K	5.94	$(1/2,3/2^-)$	$(2p_{3/2})$	0.03		1±1	
21	Ca	6.00	$(3/2)^-$		(0.02)	1.0±0.6		
42	K	6.35	$5/2^+$	$(1d_{5/2})$	1.25	6.7±1.4	7±1	
22	Ca	6.15	$(3/2,5/2)^+$		1.3	1.1±0.6	1.5±0.8	
-	Ca	6.40	$(5/2^+)$	$(1d_{5/2})$	(0.25)	1.4±0.5		
49	K	6.55	$7/2^-, T=3/2$			2±1		
-	K	6	$(5/2^+)$	$(1d_{5/2})$	(0.1)	4±1.5		
-	Ca	6.92	$(5/2^+)$	$(1d_{5/2})$	(0.09)	3.7±1.3		
-	Ca	7.70	$(5/2^+)$	$(1d_{5/2})$	(0.1)	1.5±0.9		97±1
-								
-	K	8.5						
		$\sigma^{int}(\gamma,p)$				≅430	$(E_\gamma^m$=30 MeV)	
		$\sigma^{int}(\gamma,n)$				≅80		

Notes: 1) Occupied mirror levels are placed next to each other in the table. They are combined by the square bracket in the second column. 2) In the extreme right-hand column, the curly brackets are for only the (γ, p) channel, i.e., they refer to levels of the ^{39}K nucleus. 3) The values of $\sigma^{int}(\gamma,p)$ and $\sigma^{int}(\gamma,n)$ were estimated from the data of several experiments. This is discussed in more detail in the text.

bremsstrahlung spectrum. The data on $\sigma^{int}(\gamma,p_i)$ and $\sigma^{int}(\gamma,n_i)$ obtained in Refs. 63 and 64 are given in Table XXIV.

In Ref. 64, the photon spectra were measured at θ_γ=140°, and the values given in Table XXIV for this study were obtained by multiplying the differential cross sections by 4π. The photons were detected in Ref. 63 at different angles, and the integrated partial cross sections given in Table XXIV for this experiment take into account the shape of the angular distribution of the decay photons.

The value of $\sigma^{int}(\gamma,n_0)$ given in the last column of Table XXIV was obtained on the basis of the data of Ref. 65. The values of $\sigma^{int}(\gamma,p_1)$ and $\sigma^{int}(\gamma,n_1)$ given in the third column on the right of the table were obtained by extrapolating the $\sigma(\gamma,p_1)$ and $\sigma(\gamma,n_1)$ measured in Ref. 63 to the region E_γ>24.6 MeV.

TABLE XXV. Probability of semidirect processes in integrated photonucleon cross sections of nuclei of the $1d2s$ shell and the fraction of transitions of group A ($1d2s \rightarrow 1f2p$).

Nucleus	E_γ^m MeV	Fraction of group A			Probability of semidirect processes		
		γ,p	γ,n	$\gamma,p+\gamma,n$	γ,p	γ,n	$\gamma,p+\gamma,n$
^{17}O	28	≤0.05	0.20-0.97	0.35–0.75	0.80–0.95	≥0.2	0.35–0.98
^{18}O	28	0.1–0.9	≥0.37	0.30–0.88	≤0.8	≥0.47	0.36–0.97
^{19}F	30	0.3–0.9	0.48–0.93	0.32–0.89	0.23–0.83	≥0.46	0.27–0.91
^{23}Na	30	0.47–0.94	0.90	0.65–0.92	0.17–0.31	0.60–0.71	0.34–0.47
^{24}Mg	30	0.68	0.82	0.71	0.47–0.62	0.90–0.95	0.62–0.73
^{25}Mg	28	0.53–0.83			0.20–0.60		
^{26}Mg	27	0.56–0.63			0.35–0.55		
^{27}Al	30	0.87	1.0	0.92	0.28–0.42	0.88	0.53–0.62
^{28}Si	28	0.80–0.85	0.99	0.86–0.89	0.66–0.86	0.93–0.96	0.74–0.89
^{29}Si	26	≅1.0	≅1.0	≅1.0	0.51–0.59	0.67–0.78	0.57–0.67
^{30}Si	26	≅1.0	≅1.0	≅1.0	0.57(≤0.77)	0.71–0.73	0.65–0.66
^{31}P	30	≥0.42	≅1.0	>0.60	0.16–0.21	0.80–0.85	0.37
^{32}S	29	≥0.55	≥0.93	>0.64	0.31–0.35	0.58–0.83	0.37–0.45
^{39}K	30	≅1.0	≅1.0	≅1.0	0.56	0.95	0.75
^{40}Ca	30	≥0.88	≅1.0	≥0.90	0.59-0.66	0.82-0.88	0.63–0.69

In Ref. 63, photoproton spectrometry in the region E_γ<24.6 MeV was used to determine the energy dependences of the cross sections of the (γ,p_0) and (γ,p_1) reactions and also of the cross sections for occupation of groups of states of the ^{39}K final nucleus with excitation energies in the intervals 2.8–4.2 MeV, 4.2–6.5 MeV, and 6.5–8.5 MeV. The integrated values of all these cross sections are given in the extreme right-hand column of Table XXIV.

There have been no measurements of the energy dependences of $\sigma(\gamma,n_i)$ except for $\sigma(\gamma,n_0)$ (Ref. 65) and $\sigma(\gamma,n_1)$ (Ref. 63). In Ref. 64, these dependences were determined by conversion from the experimental cross sections $\sigma(\gamma, p_i)$ (Ref. 63).

In Ref. 64, not only the semidirect components $\sigma(\gamma, p_i)$ and $\sigma(\gamma, n_i)$ but also $\sigma^{\text{int}}_{\text{s dir}}(\gamma,p)$ and $\sigma^{\text{int}}_{\text{s dir}}(\gamma,n)$ were calculated. The details of the calculations are given in Refs. 64, 66, and 67.

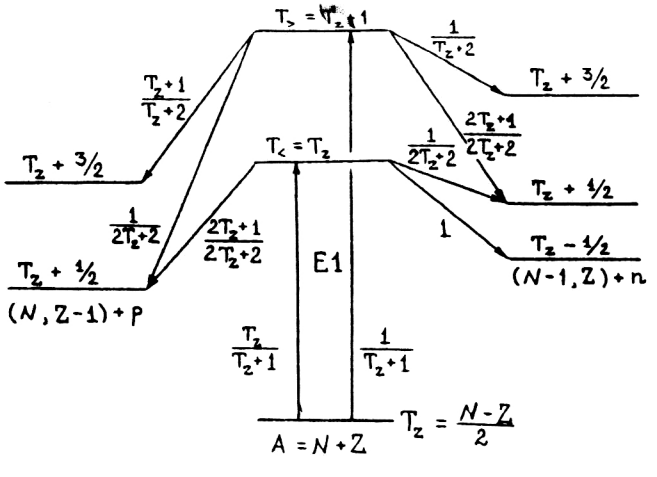

FIG. 1. Isospin scheme of excitation and nucleon decay of the giant resonance in non-self-conjugate ($N \neq Z$) nuclei. The probabilities of excitation and decay, determined by the squares of the Clebsch–Gordan isospin coefficients, are shown.

It can be seen from Table XXIV that the results of the two $(\gamma, x\gamma')$ experiments[63,64] agree with each other and with the data of Ref. 63 on proton spectrometry in the region $E_i \leq 6.4$ MeV. The levels of the final nuclei above this excitation energy decay predominantly with the emission of nucleons (the proton separation energy in the ^{39}K nucleus is 6.374 MeV, and in the ^{39}Ca nucleus it is 5.804 MeV). Therefore, only some of these decays could be separated by the

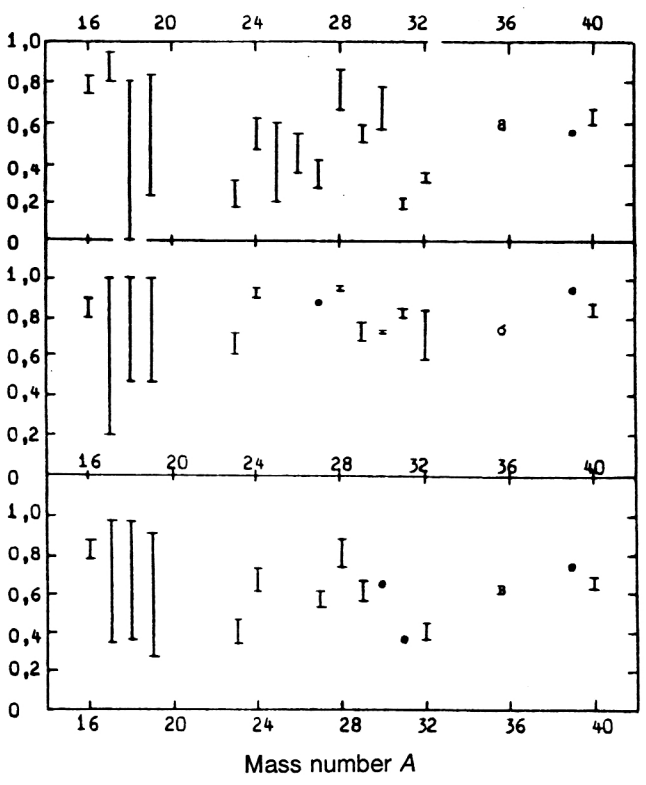

FIG. 2. Probability of semidirect decay of the giant resonance of nuclei of the $1d2s$ shell: a) (γ,p) reaction; b) (γ,n) reaction; c) (γ,N) reaction. Here, N is a proton or a neutron.

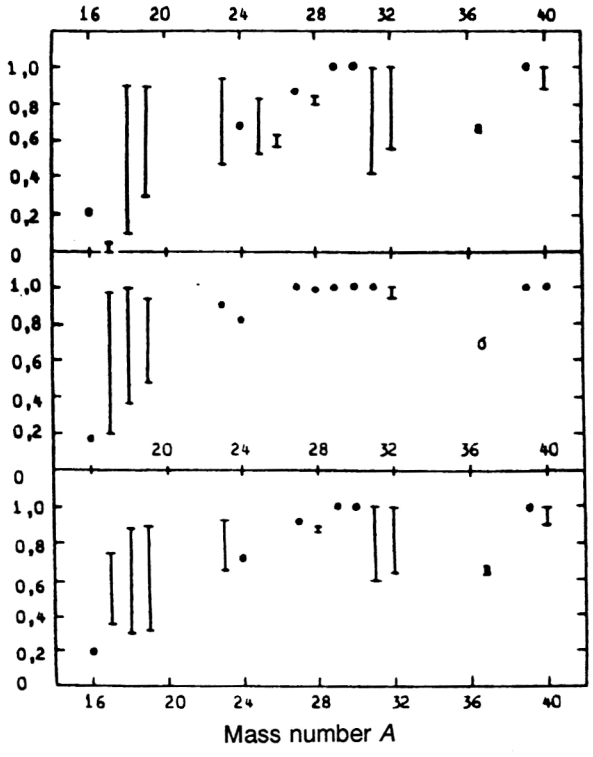

FIG. 3. Fraction of transitions of group A ($1d2s \rightarrow 1f2p$) in the giant resonance of nuclei of the $1d2s$ shell: a) (γ,p) reaction; b) (γ,n) reaction; c) (γ,N) reaction. Here N is a proton or a neutron.

detection of secondary γ rays. The decays of the highly excited states of ^{39}K and ^{39}Ca must contribute to the cross sections of the $(\gamma, 2p)$ and (γ, np) *reactions. The threshold of the* $(\gamma, 2n)$ reaction is too high (29.3 MeV) for this reaction to make a significant contribution to the photoneutron channel up to E_γ=30 MeV. A number of $(\gamma, 2p_i)$ channels were found in the experiment of Ref. 64. References to (γ, np) experiments can be found in Refs. 66 and 67. It follows from the cited studies in particular that

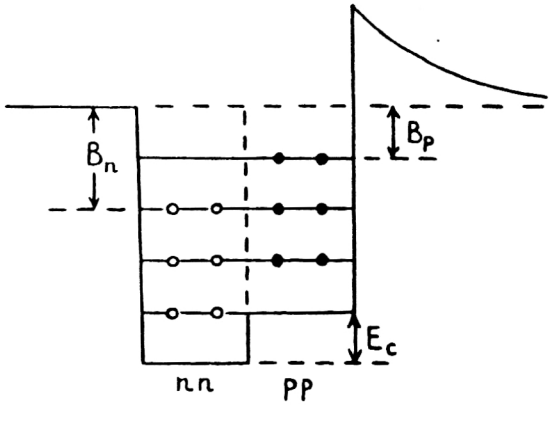

FIG. 4. Schematic representation of the potential well for protons and neutrons.

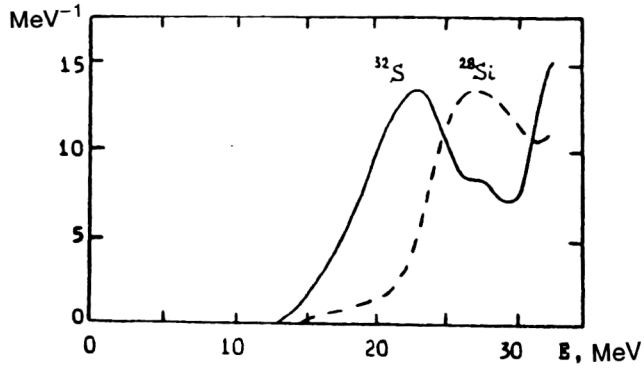

FIG. 5. Densities of $2p2h$ dipole states calculated for the ^{28}Si and ^{32}S nuclei in Ref. 42.

$$\int_0^{32} \sigma(\gamma,np)dE_\gamma \cong 7-8 \ \text{MeV}\cdot\text{mb}.$$

Bearing in mind that in accordance with Ref. 17 (see Table XXIV in this paper)

$$\int_0^{30} \sigma(\gamma,p+\gamma.np+\gamma,2p)dE_\gamma = 470\pm 40 \ \text{MeV}\cdot\text{mb}$$

and

$$\int_0^{30} \sigma(\gamma,n+\gamma,np)dE_\gamma = 88\pm 8 \ \text{MeV}\cdot\text{mb},$$

we obtain the following estimates for the integrated cross sections of the (γ,p) and (γ,n) reactions for $E_\gamma^m \leq 30$ MeV:

$$\int_0^{30} \sigma(\gamma,p)dE_\gamma \simeq 430 \ \text{MeV}\cdot\text{mb},$$

$$\int_0^{30} \sigma(\gamma,n)dE_\gamma \simeq 80 \ \text{MeV}\cdot\text{mb}.$$

The cross section $\sigma^{\text{int}}(\gamma,n)$ obtained by adding the numbers given in the third column on the right of Table XXIV is about 90 MeV·mb, and this exhausts the integrated value of the photoneutron cross section in the region E_γ<30 MeV. This means that the data of Table XXIV contain essentially complete information about the neutron decay channels of the GDR of the ^{40}Ca nucleus.

According to the data of Ref. 63, the integrated cross section for occupation of the ^{39}K levels with E_i>6.4 MeV is close to 100 MeV·mb ($E_\gamma \leq 24.6$ MeV). Only a small fraction of this value (not more than 20 MeV·mb) can be explained by the (γ,p_i) reaction channels observed in Ref. 64 in this region of E_i (see Table XXIV) and also by the $(\gamma,2p_0)$ reaction. In the $(\gamma,p\gamma')$ experiment of Ref. 64 in the region E_i>6.4 MeV the total integrated value of the unseparated (γ,p_i) cross section is more than 80 MeV·mb.

The data of Table XXIV indicate that there are no $1p \rightarrow (1d2s)$ transitions in the (γ,n) channel. In the (γ,p) channel, their fraction cannot be more than 50·100/430

TABLE XXVI. Neutron and proton separation energies B_n and B_p in the investigated nuclei of the $1d2s$ shell and the difference $\Delta_{s\,\mathrm{dir}}$ in the probabilities of semidirect processes in the (γ,n) and (γ,p) channels.

Group	Nucleus	Isospin projection T_z	B_n, MeV	B_p, MeV	$\Delta B_{np}=B_n-B_p$, MeV	$\Delta_{s\,\mathrm{dir}}$, %
	^{16}O	0	15.67	12.13	3.54	7.5±5.3
	^{24}Mg	0	16.53	11.69	4.84	13±5
I	^{28}Si	0	17.18	11.58	5.60	19±10
	^{32}S	0	15.09	8.90	6.19	38±13
	^{40}Ca	0	15.62	8.33	7.29	33±5
	^{19}F	1/2	10.43	7.99	2.44	from −37 to +77
	^{23}Na	1/2	12.42	8.79	3.63	40±11
II	^{27}Al	1/2	13.06	8.27	4.79	53±8
	^{31}P	1/2	12.31	7.29	5.02	64±4
	^{39}K	1/2	13.09	6.37	6.72	39±5
	^{17}O	1/2	4.14	13.78	−9.64	
	^{18}O	1	8.05	15.94	−7.89	
III	^{25}Mg	1/2	7.33	12.06	−4.73	
	^{26}Mg	1	11.10	14.15	−3.05	
	^{29}Si	1/2	8.48	12.33	−3.85	18±7
	^{30}Si	1	10.62	13.51	−2.89	15±6

≈12% of the integrated cross section [in the total cross section of the (γ,n) and (γ,p) reactions, this fraction does not exceed 10%].

The ground state and first two excited states of the ^{39}K and ^{39}Ca nuclei are pure nucleon holes in the subshells $1d_{3/2}$, $2s_{1/2}$, and $1f_{7/2}$, respectively, relative to the ground state of the ^{40}Ca nucleus. The occupation of these states was assumed to be entirely due to semidirect decays. The remaining ^{39}K and ^{39}Ca states either contain no hole components at all (for them, C^2S_i is equal to zero, and therefore they are not given in Table XXIV) or contain only a fraction of the spectroscopic strength of the hole excitation in the $1d_{5/2}$ and $2p_{3/2}$ subshells. The partial cross sections for excitation of the levels for which C^2S_i are not given (i =4,6,10,15,16,21,23,28,29) are entirely formed by the indirect mechanism of GDR decay.

Calculation of the semidirect components shows[64,66,67] that the levels of ^{39}K and ^{39}Ca containing an admixture of a hole in the $2p_{3/2}$ subshell (i=3,5,8,32,34) are almost entirely occupied by the indirect mechanism of GDR decay. Isobar analog pairs of ^{39}Ca and ^{39}K levels containing an appreciable fraction of the spectroscopic strength of the hole in the $1d_{5/2}$ subshell (i=18 and 22, 19 and 26, 22 and 42) of the ^{40}Ca nucleus are occupied with high probability by semidirect decays of the GDR. In the total integrated cross sections of the (γ,p) and (γ,n) reactions, the fraction of the semidirect decays is 0.59–0.66 and 0.82–0.88, respectively. In the total integrated photonucleon cross section $[\sigma^{\mathrm{int}}(\gamma,p)+\sigma^{\mathrm{int}}(\gamma,n)]$, this fraction is 0.63–0.69. All estimates correspond to the region $E_\gamma \leqslant 30$ MeV.

Finally, in Refs. 64, 66, and 67 the probability of semidirect decays in the photoabsorption cross section σ_γ was estimated for ^{40}Ca. It was found with allowance for all possible decay channels of the GDR: (γ,p), (γ,n), $(\gamma,2p)$, (γ,np), (γ,α), (γ,τ). Bearing in mind that the emission of two nucleons and composite particles (α and τ) makes the predominant contribution to the semidirect part of the photoabsorption cross section, it was found that the probability of semidirect decays in $\sigma_\gamma^{\mathrm{int}}$ is about 0.55. A similar result was also obtained in a theoretical calculation of σ_γ for ^{40}Ca made in Ref. 68. According to this calculation, the probability of semidirect decay at the maximum of the GDR is ≈0.50.

4. SYSTEMATIZATION OF THE RESULTS

Separation of the transitions to different states of the final nucleus $A-1$ showed that hole states of the initial nucleus are predominantly occupied. Assuming that this fact is directly related to the semidirect mechanism of nucleon emission from states forming the dipole resonance, it was possible to estimate qualitatively for each nucleus the corresponding contribution in the framework of the employed assumptions. This information is systematized on the right-hand side of Table XXV. We give separately the results of analysis of the experimental data on both the proton and the neutron channel. In the final column, we give the total result. Note that the total result almost exhausts the cross section of total photoabsorption.

In the left-hand part of Table XXV, we have systematized data on the contribution of dipole transitions of nucleons of the outer $1d2s$ shell to the giant resonance of the investigated nuclei. These data are also given separately for the proton and neutron channels. The total result is also given.

The results of estimates of the fraction of semidirect transitions in nuclei of the $1d2s$ shell and of the contribution of dipole transitions of nucleons of the outer $1d2s$ shell are also given in Figs. 2 and 3. These figures also give data for the ^{16}O nucleus obtained by analyzing the results of Ref. 69.

Our systematics demonstrate some interesting and sometimes unexpected facts. We shall discuss below in this section these facts and give an interpretation of them at a qualitative level (since there are no theoretical investigations of

this kind). Naturally, the analysis does not pretend to absolute completeness and in some respects may be subsequently refined or modified.

The probability of semidirect processes in the (γ,p) channel varies in the interval 0.2–0.8 with an average over the complete group of nuclei around 0.5. We note the rapid change of the probability of semidirect decay in the proton channel in going from nucleus to nucleus. These changes greatly exceed the errors in the estimates and therefore reflect the real situation.

The probability of semidirect decay in the (γ,n) channel is appreciably greater than in the (γ,p) channel (on the average by 40%) and varies in the range 0.6–1.0. For the total cross section, this probability varies from 0.4 to 0.8 with an average over all the nuclei of 0.6–0.7.

The noted significant excess of the probability of semidirect decay in the (γ,n) channel over the (γ,p) channel is essentially observed for all nuclei for which such a comparison can be made. We must here especially mention the nuclei ^{6}O, ^{28}Si, and ^{40}Ca, which have been most fully investigated in a large number of experiments and for which there are no doubts at all about the data.

At least two factors could influence such a strong difference in the probabilities of the semidirect processes in the photoneutron and photoproton channels: the difference in the thresholds (or separation energies) for the protons and neutrons, and isospin splitting of the GDR. We shall analyze both factors. Let us consider Table XXVI, where for the investigated nuclei of the $1d2s$ shell we give the separation energies of the neutrons and protons, B_n and B_p, their differences $\Delta B_{np}=B_n-B_p$, and also the differences

$$\Delta_{s\ \mathrm{dir}}=\Delta^{n}_{s\ \mathrm{dir}}-\Delta^{p}_{s\ \mathrm{dir}}$$

in the probabilities of the semidirect processes in the (γ,n) and (γ,p) reactions. The nuclei are divided into three groups: The first group contains self-conjugate $(N=Z)$ even–even nuclei with isospin projection $T_z=0$; the second group contains nuclei having one proton less than the neighboring self-conjugate nucleus, i.e., nuclei with $T_z=1/2$; the third group contains nuclei having 1–2 neutrons more than the neighboring self-conjugate nucleus.

We begin the analysis with nuclei of the first group, for which there is no isospin splitting of the GDR. For the nuclei of this group, B_n is appreciably greater than B_p, and $\Delta B_{np}(A)$ increases as A increases from 3.54 MeV for ^{16}O to 7.29 MeV for ^{40}Ca. This difference increases because of the Coulomb interaction between the protons, as a result of which the potential well for the protons in the nucleus is shallower than for the neutrons by the proton Coulomb energy $E_c=1.44Z/A^{1/3}-1.13$ MeV. This situation is shown schematically in Fig. 4. Because of the deeper potential well for the neutrons, the B branch of the GDR, associated with excitation of an inner $1p$ shell, is suppressed in the (γ,n) channel in relation to the (γ,p) channel. Since the probability of semidirect processes in the B branch of the GDR is much lower than in the A branch,[17] this leads to the observed excess of the fraction of the semidirect mechanism in the (γ,n) reaction over the (γ,p) reaction. It can also be seen from Table XXVI that with increasing ΔB_{np} there is also an increase of $\Delta_{s\ \mathrm{dir}}$. Averaging of $\Delta_{s\ \mathrm{dir}}$ for the first group of nuclei gives $\bar{\Delta}_{s\ \mathrm{dir}}\simeq 22\%$.

For the nuclei of the second group, there is approximately the same difference between B_n and B_p as for the nuclei of the first group, and this must lead to a higher fraction of semidirect processes in the (γ,n) channel. In addition, for the nuclei of the second group there exists an isospin splitting of the GDR, which also helps to increase the probability of semidirect processes in the (γ,n) reaction and to reduce it in the (γ,p) reaction. In the given case, the threshold (kinematic) and isospin factors act in the same direction, and this must lead to a larger value of $\Delta_{s\ \mathrm{dir}}$ for the second group of nuclei than for the first. The data of Table XXVI confirm this. The averaging of $\Delta_{s\ \mathrm{dir}}$ for the second group of nuclei (without allowance for the insufficiently definite data for ^{19}F) give $\bar{\Delta}_{s\ \mathrm{dir}}\simeq 45-50\%$, which is much greater than for the nuclei of the first group (22%).

We now consider why the isospin factor helps to increase the probability of semidirect processes in the (γ,n) channel in relation to (γ,p). We examine Fig. 1, which shows the scheme of isospin splitting of the GDR that arises for nuclei with nonvanishing T_z. The value of the isospin splitting (the difference between the energies $T_<$ and $T_>$ of the GDR branches), calculated in accordance with the expression of Ref. 18,

$$\Delta E=60\,\frac{T_z+1}{A}\ \mathrm{MeV}, \tag{12}$$

varies from 4.7 MeV for ^{19}F to 2.3 MeV for ^{39}K. Because of this splitting in energy, the $T_>$ and $T_<$ doorway dipole $1p1h$ states can be in a region with very different density of the dipole $2p2h$ levels, decay to which leads to the occurrence of statistical (nonsemidirect) photonucleons. The probability of occurrence of statistical nucleons is determined by the decay width $\Gamma^{\downarrow}$ (the total decay width of the giant resonance is $\Gamma=\Gamma^{\uparrow}+\Gamma^{\downarrow}$, where $\Gamma^{\uparrow}$ is the width of semidirect decay), which is determined by the relation

$$\Gamma^{\downarrow}=2\pi\overline{\langle 2p2h|V|1p1h\rangle^{2}}\rho_{2p2h}, \tag{13}$$

where $\overline{\langle\ldots\rangle^{2}}$ is the mean-square matrix element of transition of $1p1h$ states to $2p2h$ states as a result of nuclear interactions, and ρ_{2p2h} is the density of $2p2h$ dipole states. Thus, the probability of nonsemidirect decays is essentially determined by the density ρ_{2p2h}. As is shown by calculations[42] of the densities of $2p2h$ dipole states made for the ^{28}Si and ^{32}S nuclei (see Fig. 5), ρ_{2p2h} increases sharply in the region of the maximum of the GDR ($\simeq$20 MeV). By virtue of this, the $T_>$ branch of the GDR is "embedded" in a much denser background of $2p2h$ states than the $T_<$ branch. Because of this, the fraction of nonsemidirect photonucleons emitted on decay of the $T_>$ branch must be appreciably greater than the fraction of nonsemidirect photonucleons emitted on decay of the $T_<$ branch. At the same time, the $T_>$ branch is manifested to a greater degree in the (γ,p) channel, and the $T_<$ branch to a greater degree in the (γ,n) channel. This effect explains the much larger value of $\Delta_{s\ \mathrm{dir}}$ for nuclei of the second group than for the first.

We give further arguments that confirm the above conception. Analysis of the experimental data on the partial decay channels of the GDR of the nuclei ^{23}Na, ^{27}Al, ^{31}P, and ^{39}K (Refs. 23, 25, 54, 62, and 70) showed that most (60–80%) of the neutron decays of the GDR of such nuclei take place to levels with $T=0$ of the final nuclei (i.e., they arise on decay of the $T_<$ branch of the GDR), and these levels are occupied almost entirely by emission of semidirect neutrons. Further, for nuclei of the second group we observe a much smaller fraction of semidirect decays in the (γ,p) channel than for the neighboring nuclei of the first group. This follows directly from the above conception, according to which the presence of the $T_>$ branch in a region with high ρ_{2p2h} is reflected above all in an increase of the statistical decays through the proton channel. If we compare the values of ΔB_{np} and $\Delta_{s\ \mathrm{dir}}$ for nuclei of the second group, we see that, in contrast to the nuclei of the first group, growth of $\Delta_{s\ \mathrm{dir}}$ with increasing ΔB_{np} is not observed. This can be explained by the halving of the isospin splitting in going from nuclei at the beginning of the $1d2s$ shell (^{19}F) to nuclei at the end of the shell (^{39}K). The isospin factor has the greatest effect on the nuclei at the beginning of the shell and thus equalizes the values of $\Delta_{s\ \mathrm{dir}}$ for nuclei with different mass numbers.

It is important to emphasize that Fig. 5 also makes it possible to explain what at first sight seems a very strange fact—the much smaller (by a factor 2 if one considers the total photonucleon cross section) probability of semidirect processes for the ^{32}S nucleus than for the ^{28}Si nucleus. The two nuclei belong to the first group of nuclei (even–even self-conjugate nuclei) and have nearly equal mass numbers. It follows from Fig. 5 that the sharp increase in the density of the $2p2h$ states over which the doorway dipole states can be distributed occurs for the ^{32}S nucleus much lower in energy (by almost 5 MeV) than for the ^{28}Si nucleus. Essentially, for the ^{32}S nucleus the entire giant resonance is "embedded" in a dense background of such states, whereas for the ^{28}Si nucleus this happens only for the high-energy part beyond the maximum of the giant resonance.

For the nuclei of the third group, $B_p>B_n$, and in this respect the situation is the opposite of that for the nuclei of the first and second groups. If the isospin factor were absent, one could expect equalization of the probabilities of semidirect decays in the (γ,n) and (γ,p) channels for nuclei of the third group or even an excess of it in the (γ,p) channel. On the other hand, the isospin factor in this case (as in the case of nuclei of the second group) has the effect of increasing $\Delta_{s\mathrm{dir}}$. It is difficult to predict the extent to which these two factors will compensate each other and which of them will be decisive. In any case, $\Delta_{s\mathrm{dir}}$ for the nuclei of the third group must be less than for those of the second group. The data on the two investigated nuclei of the third group (^{29}Si,^{30}Si) confirm this.

We now discuss the role of the nucleons of the outer ($1d2s$) shell in the formation of the giant resonance of the investigated nuclei. In Fig. 3, we have systematized the data on the excitation probability of the A branch of the GDR. It can be clearly seen that the probability of excitation of the A branch increases with increasing mass number and that at $A\simeq 30$ the B branch has practically disappeared. The increase of the A branch with increasing mass number is the effect, predicted by the concept of "configuration splitting" of the GDR (Ref. 17), of occupation of the $1d2s$ shell with increasing number of nucleons.

Comparison of Figs. 3a and 3b shows that the B branch in the (γ,n) reaction dies away earlier than in the (γ,p) reaction. This can be explained by the fact that for the majority of the analyzed nuclei the photoneutron threshold is appreciably higher than the photoproton threshold (see Table XXVI), and this leads to an additional suppression of the B branch in the photoneutron channel.

However, it must be remembered that an appreciable fraction of decays of the group B is at excitation energies above 30 MeV (Refs. 17 and 71), i.e., outside the energy region that has been analyzed in this review. Therefore, to see the B branch in the nuclei at the end of the $1d2s$ shell and, *a fortiori*, to investigate it in detail, experiments that measure the partial photonucleon cross sections at $E_\gamma>30$ MeV are needed.

5. CONCLUSIONS

In this review, we have systematized and analyzed all the available material on the partial photonuclear cross sections of nuclei of the $1d2s$ shell ($8\leqslant Z\leqslant 20$) obtained from experiments on nucleon spectrometry and gamma-ray deexcitation ($\gamma,x\gamma'$ experiments). The total number of measured partial transitions for the 15 nuclei of this region exceeds 300. The presented systematization contains the most complete and deep information on the decay of the giant dipole resonance with occupation of individual levels of the final nuclei. Its analysis demonstrates the exceptional effectiveness of this method of investigating highly excited nuclear states. For the nuclei of the $1d2s$ shell, this analysis has revealed:

- A high probability of the semidirect mechanism of decay of the GDR, as a result of which the nucleus remains in a hole state after emission of the nucleons.
- The photoneutron channel gives particularly good information about the configuration structure of the doorway dipole states.
- There is a strong influence of the kinematic and isospin factors on the relative importance of the semidirect and statistical mechanisms of decay of the GDR.
- The shell structure of the GDR matches the conception of its "configuration splitting."[17]

All these results follow directly from the experimental data. It must be particularly emphasized that the presented experimental material opens up a unique possibility for testing modern nuclear theories. All the information about the measured partial channels is available at the Center for Data of Photonuclear Experiments of the Nuclear Physics Institute of Moscow State University (Moskva 119899, NIIYaF MGU, TsDFÉ) and can be supplied to interested persons.

At the present time, the most complete data on partial photonuclear channels are available for the nuclei of the $1d2s$ shell. It is therefore desirable to extend the experiments to nuclei of other regions and above all to the light nuclei of the $1f2p$ shell, for which the considered method may also be very effective. However, the interpretation of such data may be less certain because of the stronger disrup-

tion of the correlation between the partial cross sections and the corresponding spectroscopic factors. So far, data have been published for $(\gamma,x\gamma')$ experiments for two nuclei of the $1f2p$ shell: ^{45}Sc (Ref. 72) and ^{58}Ni (Ref. 73).

With regard to nuclei of the $1d2s$ shell, it is also difficult to regard the experiments in this region as completed. In particular, it is necessary to obtain $(\gamma,x\gamma')$ data for the isotopes ^{33,34}S, ^{35,37}Cl, and ^{36,40}Ar in order to fill the range of mass numbers $32<A\leqslant 40$. A first report of a $(\gamma,x\gamma')$ experiment on chlorine isotopes has been published.[74] It would be very helpful to have data on the neon isotopes and more accurate experiments on the isotopes of oxygen and ^{25,26}Mg. If all these data were available, there would be a much more secure basis for discussing the properties of photodisintegration of nuclei of the $1d2s$ shell in the region of the GDR that we considered in the previous section, and such data could lead to the discovery of new effects. One of the possible expected effects is an increase in the probability of semidirect processes in nuclei with closed shells. Figure 2 shows that the probability of the semidirect mechanism is apparently maximal at $A\simeq 16$, 28, and 40, i.e., at the mass numbers that correspond to closing of the $1p$ shell, the $1d_{5/2}$ subshell, and the $1d2s$ shell. However, to draw final conclusions we still need information on the nuclei with $A=17$, 18, 20–22, 25, 26, 33–38.

With regard to experiments using particle spectrometry, the data of the present review indicate the very high value of the energy dependences of the partial photoneutron cross sections for studying the shell structure of the GDR. The semidirect processes are dominant in the photoneutron cross sections. Because of this, the nature and probability of the occupied states of the final nucleus in the (γ,n) reaction give the most direct information about the subshells that participate in the excitation of the GDR. The value of such information justifies the difficulty of performing such experiments.

This work was partly supported by a grant from the Russian Foundation for Fundamental Research and a grant from the University of Russia.

[1] B. S. Ishkhanov, I. M. Kapitonov, and R. A. Éramzhyan, Fiz. Elem. Chastits At. Yadra **23**, 1770 (1992) [Sov. J. Part. Nucl. **23**, 774 (1992)].
[2] S. Fallieros and B. Goulard, Nucl. Phys. A **147**, 593 (1970).
[3] G. V. O'Reilly, D. Zubanov, and M. N. Thompson, Phys. Rev. C **40**, 59 (1989).
[4] K. Bangert, U. E. P. Berg, K. Wienhard, and H. Wolf, Z. Phys. A **278**, 295 (1976).
[5] J. G. Woodworth, K. G. McNeil, J. W. Jury *et al.*, Phys. Rev. C **19**, 1667 (1979).
[6] F. Ajzenberg-Selove, Nucl. Phys. A **460**, 1 (1986).
[7] G. Mairle, G. J. Wagner, P. Doll *et al.*, Nucl. Phys. A **299**, 39 (1978).
[8] J. W. Jury, J. D. Watson, D. Bowley *et al.*, Phys. Rev. C **32**, 1817 (1985).
[9] J. W. Jury, B. L. Berman, D. D. Faul *et al.*, Phys. Rev. C **21**, 503 (1980).
[10] J. D. Allan, J. W. Jury, R. G. Johnson *et al.*, Can. J. Phys. **53**, 786 (1975).
[11] J. W. Jury, P. C.-K. Kuo, H. R. Weller, and S. Raman, Phys. Rev. C **36**, 1243 (1987).
[12] B. J. Thomas, A. Buchnea, J. D. Jrish, and K. G. McNeil, Can. J. Phys. **50**, 3085 (1972).
[13] J. E. M. Thomson and M. N. Thompson, Nucl. Phys. A **330**, 66 (1979).
[14] E. Kerkhove, R. Van de Vyver, H. Ferdinande *et al.*, Phys. Rev. C **32**, 368 (1985).
[15] N. K. Sherman, K. H. Lokan, and R. W. Gelli, Can. J. Phys. **54**, 1178 (1976).
[16] I. M. Kapitonov, *Doctoral Dissertation* [in Russian] (Institute of Nuclear Physics, State University, Moscow, 1983).
[17] R. A. Eramzhyan, B. S. Ishkanov, I. M. Kapitonov, and V. G. Neudatchin, Phys. Rep. **136**, 229 (1986).
[18] R. Ö. Akyüz and S. Fallieros, Phys. Rev. Lett. **27**, 1016 (1971).
[19] A. Veyssière, R. Bergère, H. Beil *et al.*, Nucl. Phys. A **227**, 513 (1974).
[20] F. Ajzenberg-Selove, Nucl. Phys. A **392**, 1 (1983).
[21] F. Ajzenberg-Selove, Nucl. Phys. A **300**, 1 (1978).
[22] B. S. Ishkhanov, V. I. Mokeev, Yu. A. Novikov *et al.*, Yad. Fiz. **32**, 885 (1980) [Sov. J. Nucl. Phys. **32**, 455 (1980)].
[23] A. S. Gabelko, K. M. Irgashev, B. S. Ishkhanov *et al.*, Yad. Fiz. **44**, 1145 (1986) [Sov. J. Nucl. Phys. **44**, 741 (1986)].
[24] B. S. Ishkhanov, I. M. Kapitonov, V. I. Shvedunov *et al.*, Yad. Fiz. **33**, 581 (1981) [Sov. J. Nucl. Phys. **33**, 303 (1981)].
[25] A. S. Gabelko, K. M. Irgashev, B. S. Ishkhanov *et al.*, Vestn. Mosk. Univ. Fiz. Astron. **28**, 24 (1987).
[26] P. M. Endt and C. Van der Leun, Nucl. Phys. A **310**, 1 (1978).
[27] K. Bangert, U. E. P. Berg, G. Junghans *et al.*, Nucl. Phys. A **261**, 149 (1976).
[28] R. A. Sutton, M. N. Thompson, M. Hirooka *et al.*, Nucl. Phys. **452**, 41 (1986).
[29] B. S. Ishkhanov, I. M. Kapitonov, V. N. Orlin *et al.*, Nucl. Phys. A **313**, 317 (1979).
[30] K. M. Irgashev, B. S. Ishkhanov, I. M. Kapitonov, and I. M. Piskarev, Yad. Fiz. **46**, 689 (1987) [Sov. J. Nucl. Phys. **46**, 385 (1987)].
[31] J. E. M. Thomson and M. N. Thompson, Nucl. Phys. A **285**, 84 (1977).
[32] V. V. Varlamov, B. S. Ishkhanov, I. M. Kapitonov *et al.*, Izv. Akad. Nauk SSSR, Ser. Fiz. **43**, 186 (1979).
[33] R. L. Gulbranson, L. S. Cardman, A. Doron *et al.*, Phys. Rev. C **27**, 470 (1983).
[34] A. De Rosa, G. Inglima, M. Sandoli *et al.*, Lett. Nuovo Cimento **40**, 401 (1984).
[35] Th. Kihm, K. T. Knöpfle, H. Riedesel *et al.*, Phys. Rev. Lett. **56**, 2789 (1986).
[36] E. Kerkhove, P. Berkvens, R. Van de Vyver *et al.*, Nucl. Phys. A **474**, 397 (1987).
[37] P. P. Singh, R. E. Segel, L. Meyer-Schützmeister *et al.*, Nucl. Phys. **65**, 577 (1965).
[38] C. P. Wu, F. W. K. Firk, and T. W. Phillips, Nucl. Phys. A **147**, 19 (1970).
[39] A. S. Gabelko, Izv. Akad. Nauk SSSR, Ser. Fiz. **51**, 976 (1987).
[40] A. S. Gabelko, *Candidate's Dissertation* [in Russian] (Institute of Nuclear Physics, State University, Moscow, 1988).
[41] E. Kuhlman, K. A. Snower, G. Feldman, and M. Hindi, Phys. Rev. C **27**, 948 (1983).
[42] V. G. Kanzyuba, *Candidate's Dissertation* [in Russian] (Institute of Nuclear Physics, State University, Moscow, 1983).
[43] P. J. Ryan and M. N. Thompson, Nucl. Phys. **457**, 1 (1986).
[44] D. Zubanov, R. A. Sutton, and M. N. Thompson, Private communication (1985).
[45] R. E. Pywell, B. L. Berman, J. W. Jury *et al.*, Phys. Rev. C **27**, 960 (1983).
[46] P. M. Endt, At. Data Nucl. Data Tables, **19**, 23 (1977).
[47] U. R. Arzibekov, A. S. Gabelko, M. Kh. Zhalilov *et al.*, Yad. Fiz. **45**, 907 (1987) [Sov. J. Nucl. Phys. **45**, 562 (1987)].
[48] L. Zalcman, J. E. M. Thomson, and M. N. Thompson, *Intern. Conf. on Photonucl. React. and Appl. Asilomar, Summaries of Contr. Papers* (1973), p. 2B12-1.
[49] H. Tsubota, N. Kawamura, S. Oikawa *et al.*, J. Phys. Soc. Jpn. **35**, 330 (1973).
[50] E. Kerkhove, H. Ferdinande, P. Van Otten *et al.*, Phys. Rev. C **31**, 1071 (1985).
[51] R. W. Gellie, K. H. Lokan, and N. K. Sherman, *Intern. Conf. on Photonucl. React. and Appl. Asilomar, Summaries of Contr. Papers* (1973), p. 2B13-1.
[52] C. P. Cameron, R. D. Ledford, M. Potokar *et al.*, Phys. Rev. C **22**, 397 (1980).
[53] U. R. Arzibekov, *Candidate's Dissertation* [in Russian] (Institute of Nuclear Physics, State University, Moscow, 1987).
[54] U. R. Arzibekov, A. S. Gabelko, B. S. Ishkhanov *et al.*, Yad. Fiz. **47**, 903 (1988) [Sov. J. Nucl. Phys. **47**, 575 (1988)].
[55] B. S. Ishkhanov, I. M. Kapitonov, V. G. Shevchenko, and B. A. Yur'ev, Phys. Lett. **9**, 162 (1964).
[56] V. V. Varlamov, B. S. Ishkhanov, I. M. Kapitonov *et al.*, Yad. Fiz. **28**, 590 (1978) [Sov. J. Nucl. Phys. **28**, 302 (1978)].

[57] J. E. M. Thomson, M. N. Thompson, and R. J. Stewart, Nucl. Phys. A **290**, 14 (1977).
[58] U. R. Arzibekov, A. S. Gabelko, and M. Kh. Zhalilov *et al.*, Izv. Akad. Nauk UzSSR, Ser. Fiz.-Mat. Nauk No. 2, 52 (1986).
[59] U. R. Arzibekov, B. S. Ishkhanov, I. M. Kapitonov, and I. M. Piskarev, Yad. Fiz. **44**, 1124 (1986) [Sov. J. Nucl. Phys. **44**, 727 (1986)].
[60] W. M. Mason, N. W. Tanner, and G. Kernel, Nucl. Phys. A **138**, 253 (1969).
[61] B. S. Ishkhanov, I. M. Kapitonov, V. G. Kanzyuba *et al.*, Nucl. Phys. A **405**, 287 (1983).
[62] U. R. Arzibelkov, A. S. Gabelko, M. Kh. Zhalilov *et al.*, Izv. Akad. Nauk SSSR, Ser. Fiz. **51**, 134 (1987).
[63] D. Brajnik, D. Jamnik, G. Kernel *et al.*, Phys. Rev. C **9**, 1901 (1974).
[64] A. S. Gabelko, M. Kh. Zhalilov, B. S. Ishkhanov *et al.*, Vestn. Mosk. Univ. Ser. Fiz. Astron. **27**, 43 (1986).
[65] C. P. Wu, J. E. E. Baglin, F. W. K. Firk, and T. W. Phillips, Phys. Lett. B **29**, 359 (1969).
[66] A. S. Gabelko, M. Kh. Zhalilov, B. S. Ishkhanov, and I. M. Kapitonov, "Giant dipole resonance of nuclei with neutron number $N=20$," Paper deposited at VINITI, No. 6142-V86 [in Russian] (Moscow, 1986).
[67] M. Kh. Zhalilov, *Candidate's Dissertation* [in Russian] (Institute of Nuclear Physics, State University, Moscow, 1986).
[68] F. A. Zhivopistsev, B. S. Ishkhanov, V. N. Orlin, and V. I. Shvedunov, Yad. Fiz. **26**, 754 (1977) [Sov. J. Nucl. Phys. **26**, 397 (1977)].
[69] J. Th. Caldwell, Ph.D. thesis (Preprint, University of California, UCRL-50287, 1967).
[70] U. R. Arzibekov, A. S. Gabelko, M. Kh. Zhalilov *et al.*, Yad. Fiz. **42**, 1059 (1985) [Sov. J. Nucl. Phys. **42**, 668 (1985)].
[71] B. S. Ishkhanov, I. M. Kapitonov, V. G. Neudachin *et al.*, Usp. Fiz. Nauk **160**, 57 (1990) [Sov. Phys. Usp. **33**, 204 (1990)].
[72] B. S. Ishkhanov, I. M. Kapitonov, and I. A. Tutyn', Yad. Fiz. **56**, No. 12, 263 (1993) [Phys. At. Nucl. **56**, 1774 (1993)].
[73] B. S. Ishkhanov, I. M. Kapitonov, and I. A. Tutyn', Yad. Fiz. **56**, No. 8, 1 (1993) [Phys. At. Nucl. **56**, 991 (1993)].
[74] B. S. Ishkhanov, I. M. Kapitonov, and I. A. Tutyn, *4th Intern. Conf. on Selected Topics in Nuclear Structure, Contributions*, Dubna (1994), p. 51.

Translated by Julian B. Barbour